CARACTERITZACIÓ NUTRICIONAL, METABÒLICA I EPIGENÈTICA DE LES NEOPLÀSIES MALIGNES DE CÈL·LULES B DE NOU DIAGNÒSTIC (SYN19/04): DADES PRELIMINARS

J. Bargay[1], J. Olivares[2], J. Borràs[1,3], C. Bouzas[4], X. Capó[4], A. Cladera[1], R. del Campo[1], C.M. Mascaró[4], C. Melià[1,3], M. Monserrat[4], M. Quetglas[4], S. Tejada[5], J.A. Tur[4], A. Sureda[4]

[1]Hospital Universitari Son Llàtzer, Servei d'Hematologia; [2]Hospital Universitari Son Llàtzer, Servei d'Endocrinologia; [3]Institut d'Investigació de les Illes Balears (IdISBa); [4]Universitat de les Illes Balears. Grup en Nutrició Comunitària i Estrès Oxidatiu; [5]Universitat de les Illes Balears. Grup en Neurofisiologia. Departament de Biologia.

*Email: catalina.melia@hsll.es

INTRODUCCIÓ I OBJECTIUS

Les neoplàsies malignes de les cèl·lules B conformen un grup heterogeni de malalties neoplàsiques on el seu origen és la proliferació descontrolada de cèl·lules B del sistema immunitari. Les neoplàsies de les cèl·lules B juntament amb les diferents modalitats de tractament que pot arribar a precisar el pacient al llarg del curs afecten negativament en l'estat nutricional, metabòlic i bioquímic del pacient, i no és infreqüent el desenvolupament de desnutrició, situació que compromet l'evolució, la resposta al tractament i la qualitat de vida del pacient. El present estudi pretén aprofundir en el coneixement dels factors fisiopatològics que acompanyen a les neoplàsies de cèl·lula B.

MATERIAL I MÈTODES

Des de l'inici del reclutament el març del 2021, s'han reclutat 25 pacients amb neoplàsies malignes de cèl·lules B de nou diagnòstic. A aquests pacients s'ha analitzat en condicions basals i abans de començat el tractament amb quimioteràpia els paràmetres bioquímics generals i marcadors d'estrès oxidatiu a plasma. Aquests valors s'han comparat amb 25 pacients de característiques semblants d'edat, sexe i índex de massa corporal però sense neoplàsies. Les diferències entre els dos grups s'han analitzat per mitjà d'una t-Student de dades desaparellades (* diferències $p<0.05$).

Característiques generals

	SYN (n=25)	Control (n=25)	T-Student
	Mitja ± error	Mitja ± error	
Edat (anys)	63.3 ± 2.41	64.3 ± 0.655	0.674
Pes (kg)	74.1 ± 2.79	76.3 ± 11.7	0.480
Alçada (m)	1.64 ± 0.018	1.60 ± 0.019	0.202
IMC (kg/m²)	27.7 ± 0.957	29.6 ± 0.376	0.051
Pressió sanguínia sistòlica (mmHg)	133.1 ± 3.95	140.2 ± 3.88	0.203
Pressió sanguínia diastòlica (mmHg)	76.7 ± 3.09	80.0 ± 1.54	0.320
Glucosa (mg/dL)	120.6 ± 13.1	109.1 ± 3.63	0.374
Triglicèrids (mg/dL)	195.4 ± 34.1	138.5 ± 13.0	0.106
HDL-colesterol (mg/dL)	37.2 ± 3.43	45.4 ± 2.19*	**0.044**
LDL-colesterol (mg/dL)	91.1 ± 7.4	114.3 ± 6.42	0.841
Colesterol total (mg/dL)	161. 3 ± 9.01	187.9 ± 6.39*	**0.018**
AST (U/L)	39.1 ± 8.96	19.9 ± 1.01*	**0.029**
ALT (U/L)	35.2 ± 7.83	22.7 ± 3.31	0.128
GGT (U/L)	107.3 ± 42.0	27.6 ± 4.75	**0.043**
Hematocrit (%)	36.4 ± 1.22	41.9 ± 0.425*	**< 0.001**
Plaquetes (10⁹/L)	266.8 ± 35.0	232.7 ± 10.2	0.325

IMC, Índex de massa corporal; HDL-colesterol, lipoproteïna de alta densitat; LDL-colesterol, lipoproteïna de baixa densitat; AST, aspartat aminotransferasa; ALT, alanina aminotransferasa; GGT, gamma glutamil transferasa.

Diagnòstic de les neoplàsies malignes de cèl·lules B

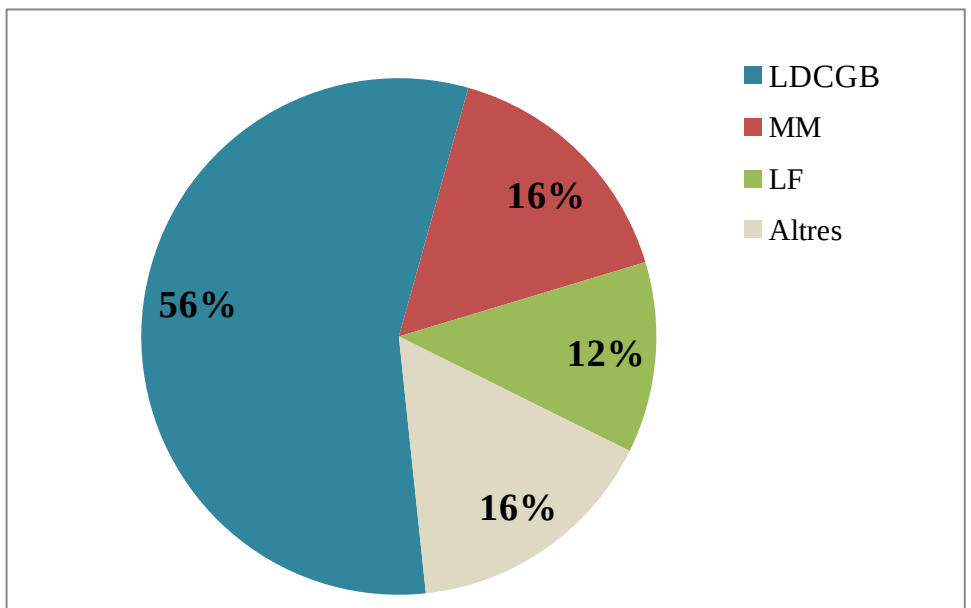

LDCGB, limfomes difusos de cèl·lula gran B; MM, mielomes múltiples; LF,limfomes fol·liculars

Activitat catalasa, superòxid dismutasa i mieloperoxidasa

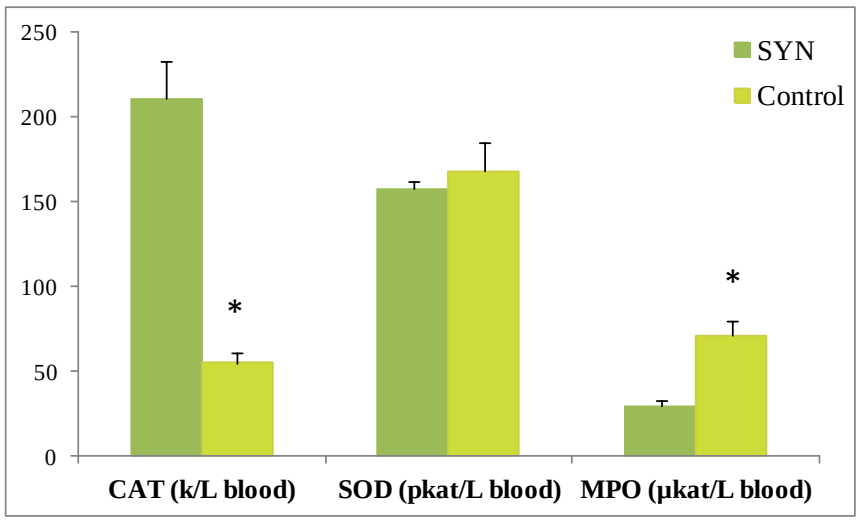

Nivells de malondialdehid

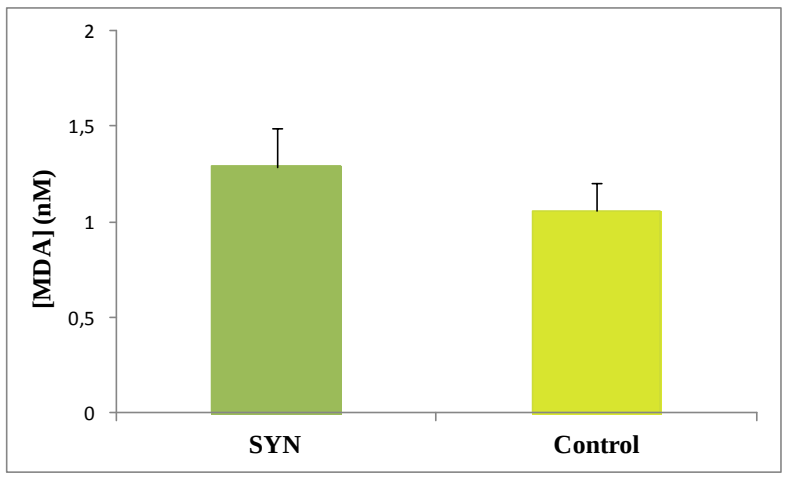

RESULTATS

Dels 25 pacients reclutats, un 56% són limfomes difusos de cèl·lula gran B; un 16% són mielomes múltiples; un 12% limfomes fol·liculars i la resta, altres diagnòstics. Els pacients presenten valors més elevats de aspartat aminotransferasa i gamma glutamil transferasa i valors més baixos de HDL-colesterol, colesterol total i hematocrit que el grup control. A més, els pacients presentaren una major activitat catalasa plasmàtica i una menor activitat mieloperoxidasa, mentre que l'activitat superòxid dismutasa i els nivells de malondialdehid foren semblants entre els dos grups.

CONCLUSIONS

Els pacients amb neoplàsies malignes de les cèl·lules B presenten alteracions de paràmetres bioquímics quan es comparen amb persones de característiques semblants però sense aquestes patologies. A mesura que es completi el reclutament i seguiment dels pacients es podrà aprofundir sobre la relació que existeix entre l'estat nutricional, metabòlic i epigenètic a les neoplàsies malignes de les cèl·lules B.

Agraïments:
Aquest projecte s'ha pogut dur a terme gràcies al finançament per part dels projectes intramurals IdISBa del programa SYNERGIA, baix el codi SYN19/04.

A bench-to-bedside approach to overcome PDAC resistance

Catalina M Perelló-Reus[1], Lesly Ibargüen-González[1], Alba Gómez[1], Juan-José Segura-Sampedro[2], Rafael Morales[2], and Carles Barceló[1]

[1]Translational Pancreatic Cancer Oncogenesis Group,; [2]Advanced Oncologic Surgery and m-Health group,
Health Research Institute of the Balearic Islands (IdISBa)

Background and aims

Pancreatic ductal adenocarcinoma (PDAC) represents the most deadly cancer. Current therapeutic strategies are ineffective to treat PDAC and almost all patients will die within five years after diagnose. PDAC resistance is mainly caused by the activity of a tumor stem cell population (PDAC-SC) that hold the capacity to regenerate the tumor after surgery/chemotherapy. However, the biology of these tumor stem cells remains poorly characterized, which hampers the development of better treatment options. Therefore, tractable methods to identify pathways involved in pancreatic stemness and tumorigenesis are urgently needed. In this project, we aim to dissect the influence of main mutated pathways in PDAC on the self-renewal and tumorigenic potential of PDAC stem cells.

Methodology

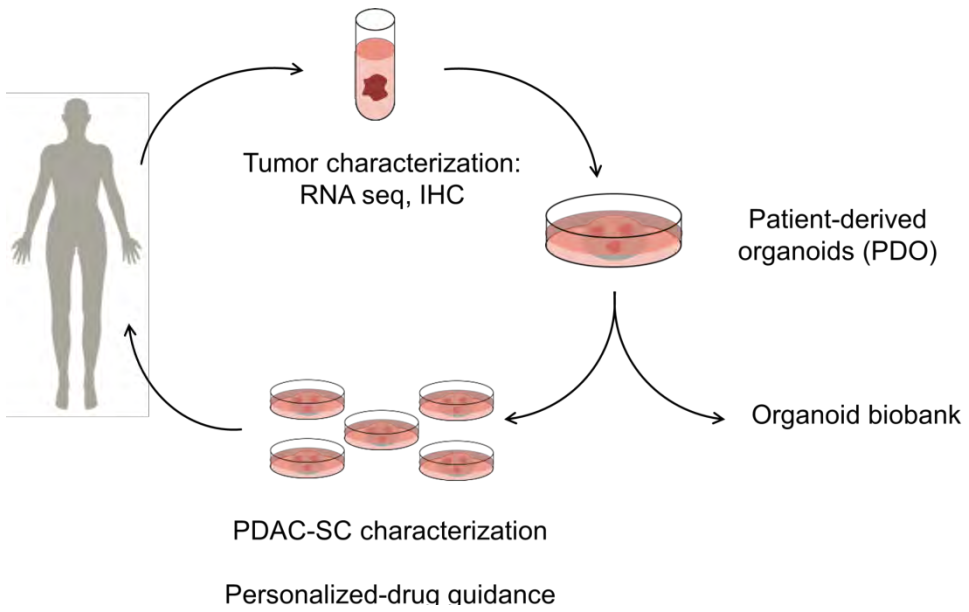

PDAC patient derived organoids (PDOs) will be generated from either fresh or cryopreserved tumor resection. In parallel, the tumors wil be characterized histologically and its mutational landscape will be analyzed by RNAseq. Once generated, PDOs will be used to unravel patient-specific PDAC-SC characteristics and to guide drug treatment in a precision medicine approach. In addition, PDOs can be cryopreserved and can serve as a living biobank for pancreatic cancer.

Figure 1. Schematic representation of the workflow.
IHC: immunohistochemistry, PDAC-SC: Pancreatic tumor stem cells

Results

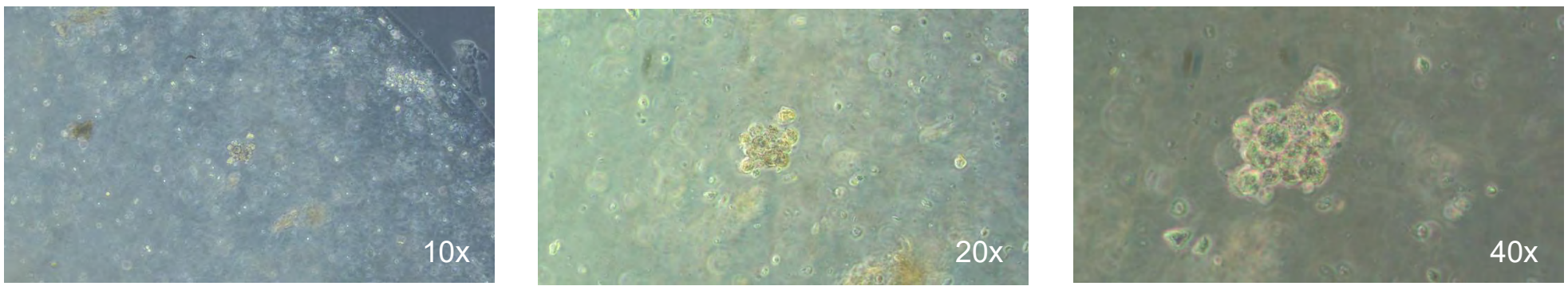

Figure 2. Representative images of PDOs. Bright field images.Optical Microscope ZEISS Axio Vert.A1

We are establishing a comprehensive collection of PDOs representative of PDAC clinical spectra embedded in a 3D matrix. Currently, we have obtained >10 tumors from patients diagnosed with PDAC that undergo a duodenum-pancreatectomy (CPD) or total duodenum-pancreactomy (DPT).

Conclusions

Patient-derived organoids open the gate to perform a “Real-time” drug guidance for PDAC patients and vulnerabilities to chemiotherapy resistance. This new approach can pave the way towards a new paradigm for precision medicine in PDAC.

Funding

Illes Sostenibles
MINISTERIO DE CIENCIA E INNOVACIÓN
Instituto de Salud Carlos III

Characterization of the cellular effects of antipsychotic phenothiazines in glioblastoma cells: Study of the cooperative potential with temozolomide

Lucía Ferro[1,3], Guillem Ramis[1,3,4], Priam Villalonga[1,2,3] and Silvia Fernandez[1,2,3].

[1]Cancer Cell Biology Laboratory, Institut Universitari d'Investigació en Ciències de la Salut (IUNICS), [2]Departament de Biologia Fonamental i Ciències de la Salut, Universitat de les Illes Balears (UIB), [3]Institut d'Investigació Sanitària Illes Balears (IdISBa), Palma, Illes Balears (Spain), [4]Cellomics Unit, IUNICS-UIB.

BACKGROUND

Glioblastoma (GBM) is the most common and aggressive primary brain tumor [1].

Patients end up being **resistant** to multimodal treatment, which implies surgery followed by radiotherapy and chemotherapy with temozolomide (TMZ). GBM patients have a median survival of **15 months**[2].

An 88% of GBM present aberrant PI3K-AKT-mTOR signaling pathway activation.

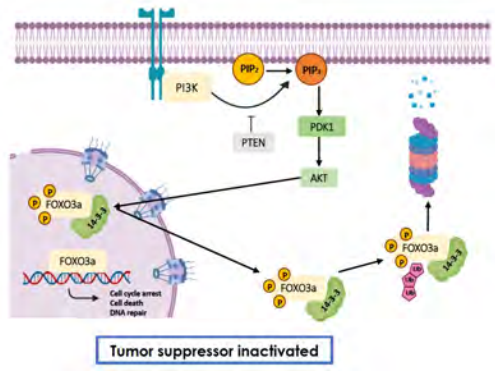

This fact implies the phosphorylation and, subsequently, **FOXO3a** nuclear export. This protein acts as a **tumor suppressor**, but it is inactivated in the vast majority of GBM[3].

Need and **urgency** of developing an effective therapeutic strategy

Drug repositioning

Antipsychotic phenothiazines

Chlorpromazine (CPZ) | **Thioridazine (TRD)**

OBJECTIVES

Evaluate the therapeutic potential of TRD and CPZ alone or in combination with TMZ, in GBM cells.

Study the cellular and molecular effect of TRD and CPZ in GBM cells.

RESULTS

Cell viability and adjuvant potential

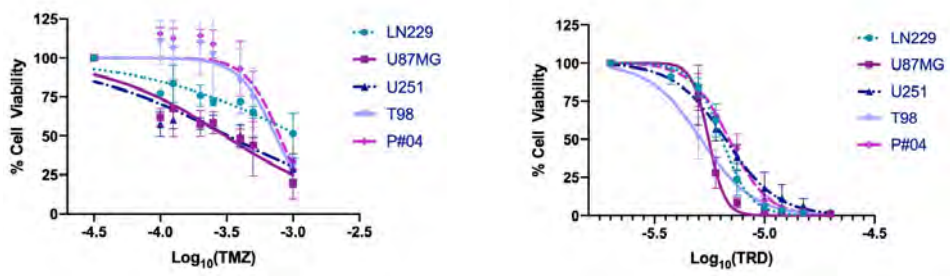

Figure 1. TRD and TMZ reduce cell viability in human GBM cell lines and in primary GBM cultures. Dose-response curves for TRD and TMZ. The indicated cell lines were treated with serial 1: 2 dilutions of the drugs, starting from a concentration greater than 20 µM. The data shown in the isobolograms correspond to the means ± SD of two independent experiments.

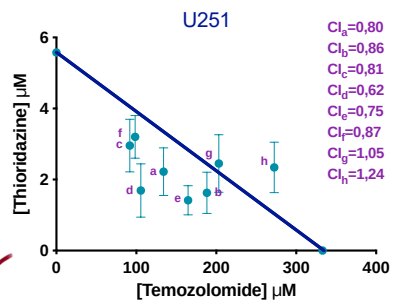

Figure 2. Synergistic effect of TRD combination with TMZ in U251 GBM cell line. GBM cell lines and patient-derived primary cell-line were treated with TMZ and TRD/CPZ at fixed combination ratios (1:1, 1:2, 2:1, 1:3, 3:1, 1:5, 5:1 and 1:10 and). The data shown in the isobolograms correspond to the means ± SD of two independent experiments.

Cellular and molecular effects

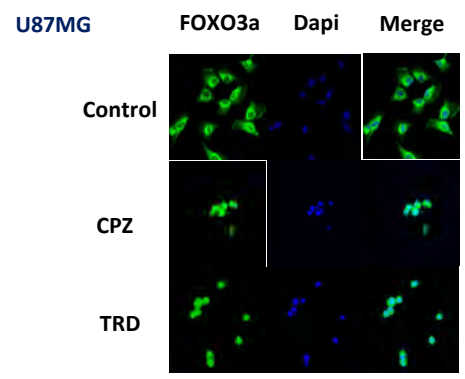

Figure 3. TRD and CPZ prevent FOXO3a nuclear export. GBM cells grew on coverslips and were treated with TRD or CPZ at 10 µM for 3h, except control cells. Then cells were fixed and labeled with an antibody specific for FOXO3a (green) and with DAPI (blue), which stains the nuclei. The images were then obtained with a confocal microscope.

Figure 4. TRD induces an increase in p27 protein levels in a time-dependent manner. Western-Blot analysis of the p27 protein in the LN229 cell line. This GBM cell line was treated with TRD at 10 µM at different times (4h, 8h, 16h and 24h). α-tubulin was used as a loading control.

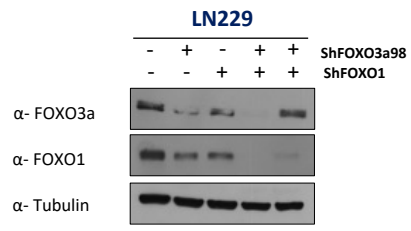

Figure 5. Knockdown of FOXO3a, FOXO1 and double-knockdown of both FOXO3a/FOXO1 mediated by recombined shRNA in lentiviral particles. FOXO3a and FOXO1 protein levels in control cells and in four LN229 clones analyzed by Western-Blot.

CONCLUSIONS

- Antipsychotic phenothiazines **decrease** GBM cell **viability**.
- Almost all **combinations** (TMZ + CPZ/TRD) are **synergistic** in GBM cells, even in TMZ-resistant cell lines or patient cells.
- Antipsychotic phenothiazines **prevent FOXO3a** nuclear **export** and **activate** its **function** by modulating the expression of FOXO3a target genes.

These results suggest the **potential** of TRD and CPZ as co-adjuvant drugs for GBM treatment.

REFERENCES

1. Maher, E. A. *et al.* Malignant glioma: genetics and biology of a grave matter. *Genes Dev.* **15**, 1311–1333 (2001).
2. Friedman, H. S., Kerby, T. & Calvert, H. Temozolomide and Treatment of Malignant Glioma. *Clin. Cancer Res.* **6**, (2000).
3. Fruman, D. A. *et al.* The PI3K Pathway in Human Disease. *Cell* **170**, 605–635 (2017).

Figures were designed with Biorender web page.

Questions and comments: lucia.ferro@uib.es

Caracterització i anàlisi de vesícules extracel·lulars de pacients afectats per càncer de colon. Array de ARNm a aspirat del lumen intestinal a colonoscòpia exploratòria.

Marina Alorda-Clara[1], Marita G. Trelles-Guzman[2], Jorge Sastre-Serra[1,3], Jordi Oliver[1,3], Daniel G. Pons[1], Pilar Roca[1,3], Jose Reyes[1,2]

1-Grup Multidisciplinar d'Oncologia Translacional, Institut Universitari d'Investigació en Ciències de la Salut (IUNICS), Universitat de les Illes Balears, Institut d'Investigació Sanitària de les Illes Balears (IdISBa), Palma, Espanya. 2-Servei Aparell Digestiu. Hospital Comarcal d'Inca, Illes Balears. 3-CIBER Fisiopatología Obesidad y Nutrición (CB06/03), Instituto de Salud Carlos II, Madrid, Espanya.

Introducció

El càncer de colon és el tercer càncer més comú en el món. Les vesícules extracel·lulars són secretades per les cèl·lules i contenen diferents molècules al seu interior. Participen en la comunicació intercel·lular, proliferació, invasió, migració, transició epiteli-mesènquima i en la formació del nínxol premetastàsic. L'objectiu va ser extreure, caracteritzar i analitzar les vesícules extracel·lulars de l'aspirat del lumen intestinal de pacients sotmesos a una colonoscòpia exploratòria per sospita de patologia colorectal.

Materials i Mètodes

Aspirat lumen intestinal

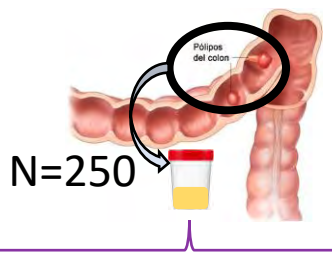

Sense patologia (Control)

Pòlips (Baix/Alt Risc)

Neoplàsia

Vesícules extracel·lulars

Caracterització: Microscopia de forces atòmiques

Extracció macromolècules

Array ARNm: normalització RMA (llibreria *oligo* de *Bioconductor*); expressió diferencial gens (llibreria *limma* de *Bioconductor*); funcions biològiques alterades (*GSEA*)

Resultats

Figura 1

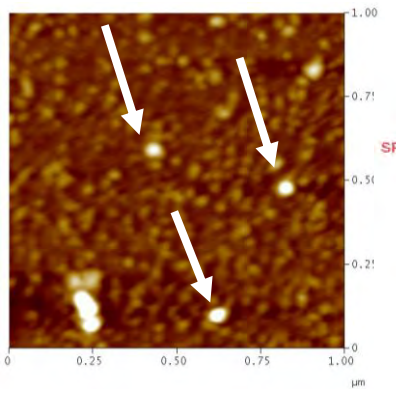

Figura 2

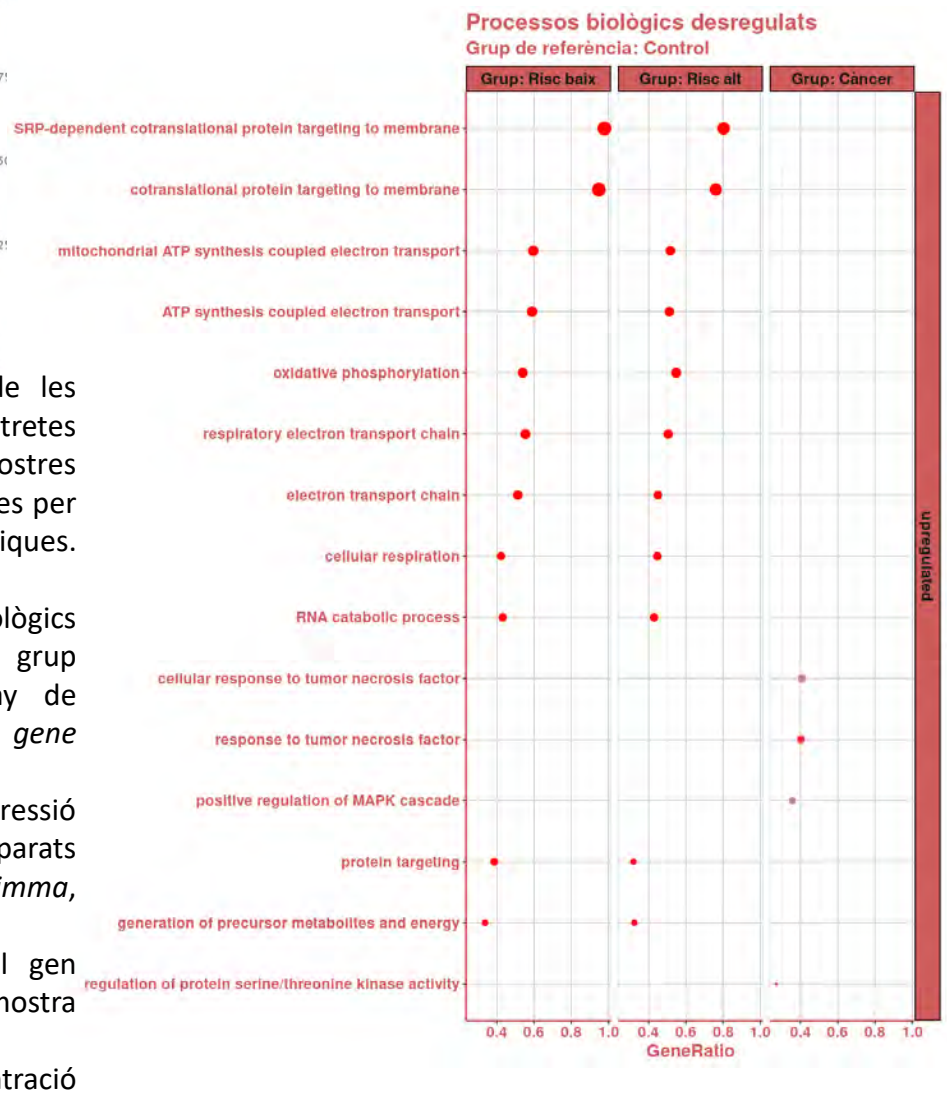

Figura 3

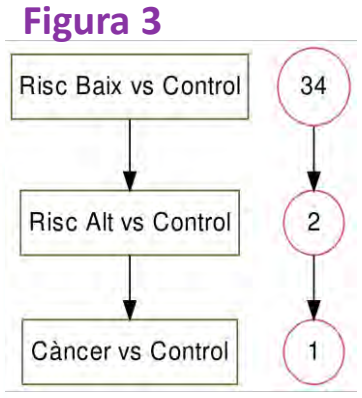

Figura 4

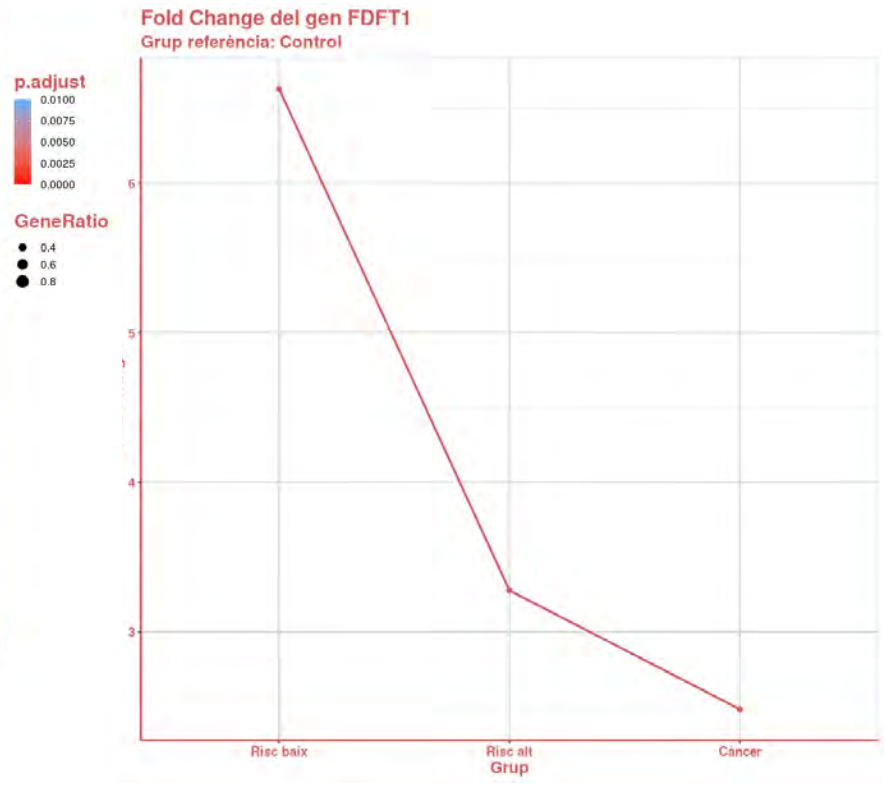

Taula 1

	Mitja ± SEM
ARN	150 ± 24,8 ng/µL
ADN	22,2 ± 4,90 ng/µL
Proteïna	0,72 ± 0,10 µg/µL

Figura 1. Caracterització de les vesícules extracel·lulars extretes per ultracentrifugació de mostres d'aspirat intestinal observades per microscopi de forces atòmiques. Ø 70-100 µm

Figura 2. Processos biològics desregulats respecte al grup control obtinguts a l'array de ARNm i posterior estudi de *gene set enrichment*.

Figura 3. Esquema de l'expressió de gens diferencials comparats amb el grup control (*limma*, *Bioconductor*).

Figura 4. *Fold change* del gen FDFT1 dels tres tipus de mostra respecte al grup control.

Taula 1. Mitja de la concentració en ng/µL de ARN i ADN i en µg/µL de proteïna obtingudes per el mètode de Tri Reagent (N=23).

Conclusió

L'anàlisi de les vesícules extracel·lulars obtingudes de l'aspirat del lumen intestinal podria suposar un gran avanç en el coneixement del càncer de colon i en la recerca de nous biomarcadors de diagnòstic i/o prognòstic d'aquesta malaltia, així com avançar en l'estudi de metodologies destinades a una medicina personalitzada.

Agraïments

HCIN Hospital Comarcal d'Inca

Universitat de les Illes Balears

Fundació Universitat Empresa de les Illes Balears

Projecte CINUIB

Els autors agraeixen al doctor Aarne Fleischer de la Plataforma de Genòmica (IdISBa) per la realització del array de ARNm i Josep Muncunill del Servei Bioinformàtic (IdISBa) per l'assistència amb les dades de l'array de ARNm.

UTILIDAD DEL PHI COMO PARÁMETRO DIAGNÓSTICO DE CÁNCER DE PRÓSTATA E IMPACTO EN LA DECISIÓN DE TOMA DE BIOPSIAS PROSTÁTICAS

Aizpiri Antoñana, L. [1]; Guimerà García, J. [1]; Muñoz Vélez, D. [1]; Parera Rosselló, M. M.[2]; Peraire Lores, M. [1]; Vega Vega, C. A. [1]; Casu Casu, V. C. [1]; Benito García, P. [1]; Pieras Ayala, E. C. [1]

[1]Servicio de Urología, Hospital Universitario Son Espases, Palma.

[2]Servicio de Análisis Clínicos, Hospital Universitario Son Espases, Palma.

INTRODUCCIÓN Y OBJETIVOS

La principal limitación del PSA como marcador para el cribaje de cáncer de próstata es su baja especificidad. El “Prostate Health Index” (PHI) se ha sugerido como un marcador sérico de mayor especificidad para este fin.

El objetivo principal de este estudio es validar la utilidad del PHI como marcador sérico para el diagnóstico de cáncer de próstata. El objetivo secundario es demostrar la relación del PHI con el grado histológico del adenocarcinoma de próstata.

MATERIALES Y MÉTODOS

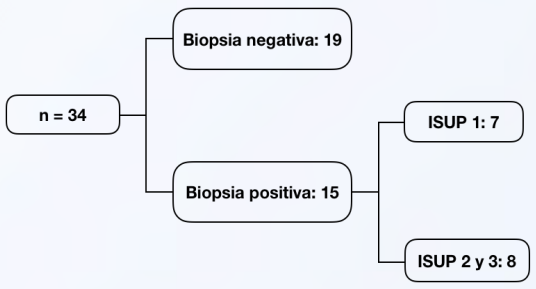

Se ha seleccionado una muestra de 34 pacientes de entre 45 y 75 años sometidos a su primera biopsia transrectal de próstata, con valores de PSA total entre 4-10 ng/mL y tacto rectal no sospechoso. Los criterios de exclusión son los siguientes: tratamiento con inhibidores de la 5-alfa-reductasa, antecedentes de biopsias prostáticas e infección del tracto urinario reciente.

Se analizaron los valores séricos de PSA, PSA libre y PHI previos a la biopsia prostática. Evaluamos el rendimiento del PSA, índice de PSA y PHI empleando el análisis de discriminación mediante curvas ROC. Asimismo, estudiamos la posible relación del PHI con el grado histológico en la biopsia mediante el análisis estadístico ANOVA.

RESULTADOS

15 pacientes (44%) fueron diagnosticados de cáncer de próstata. 7 pacientes (20%) obtuvieron una puntuación Gleason 6 (grado ISUP 1) y 8 pacientes (23%) fueron clasificados como Gleason 7 (grados ISUP 2 y 3).El PHI presentó un área bajo la curva (AUC) de 0.90; frente al PSA y el índice de PSA, de 0.53 y 0.74, respectivamente, demostrando diferencia estadísticamente significativa (p ≤ 0’05).

Para un valor de corte de PHI de 35, la sensibilidad fue del 86% y la especificidad del 73% para la detección del cáncer de próstata. El valor de PHI en los pacientes con resultado negativo en la biopsia fue de 27.7, siendo de 49.3 y 60.2 para grado ISUP 1 y grado ISUP2-3, respectivamente (p<0’05).

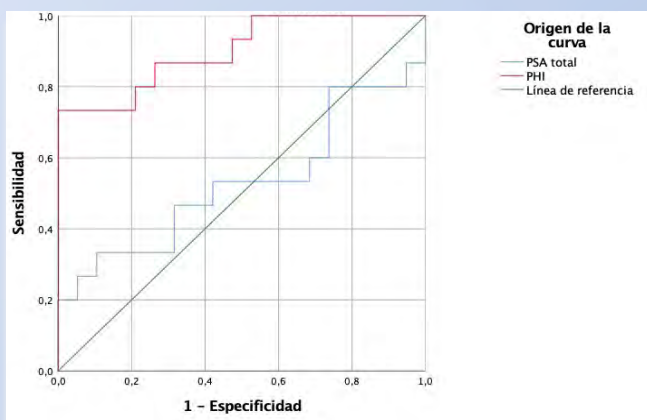

Variables de resultado de prueba	Área	Desv. Error[a]	Significación asintótica[b]	95% de intervalo de confianza asintótico	
				Límite inferior	Límite superior
PSA total	,530	,107	,768	,319	,740
PHI	,902	,053	,000	,797	1,000

a. Bajo el supuesto no paramétrico
b. Hipótesis nula: área verdadera = 0,5

CONCLUSIONES

El PHI demostró superioridad frente al valor de PSA y el índice de PSA para la detección de cáncer de próstata. El valor de PHI se relacionó con el grado histológico del cáncer de próstata.

Contacto: Laura Aizpiri
e-mail: lauraaizpiri@gmail.com

Estudio inmunohistoquímico de proteínas antioxidantes en cáncer de colon

Margalida Torrens-Mas[1], Melany Oliva-Sobrado, Alexandra Gene[2], Jose Reyes[2], Daniel Gabriel Pons[2], Jordi Oliver[2,3], Jorge Sastre-Serra[2,3], Marta González-Freire[1], Guillem Artigues[4], Pilar Roca[2,3]

1 Grupo de Patologías Vasculares y Metabólicas, Instituto de Investigación Sanitaria de las Islas Baleares (IdISBa), Palma, España.

2 Grupo Multidisciplinar de Oncología Traslacional, Institut Universitari d'Investigació en Ciències de la Salut (IUNICS), Universitat de les Illes Balears, Institut d'Investigació Sanitària de les Illes Balears (IdISBa), Palma, España.

3 CIBER Fisiopatología Obesidad y Nutrición (CB06/03), Instituto de Salud Carlos III, Madrid, España.

4 Grup d'Investigació en Salut Pública de les Illes Balears, Instituto de Investigación Sanitaria de las Islas Baleares (IdISBa), Palma, España.

Introducción

El cáncer de colon es el tumor más frecuentemente diagnosticado en España considerando ambos sexos.

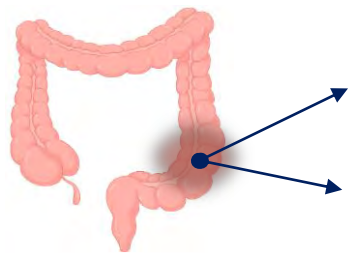

Se ha descrito que la inflamación es un factor de riesgo que favorece la aparición y el desarrollo de este cáncer.

El <u>objetivo</u> de este estudio fue analizar los niveles de diversas proteínas antioxidantes en tejidos <u>sano</u>, <u>inflamado</u> y <u>tumoral</u> de pacientes de cáncer de colon.

Materiales y métodos

Se reclutaron pacientes de cáncer colorrectal que tuvieran que someterse a una intervención quirúrgica, en la que se recogieron muestras de tejido normal, tejido tumoral y tejido inflamatorio peritumoral. Se analizaron los niveles de distintas proteínas antioxidantes (UCP2, SIRT3 y SOD2) por inmunohistoquímica. Tres evaluadores independientes valoraron la intensidad obtenida en los distintos cortes. Finalmente, se analizó la supervivencia de pacientes de cáncer colorrectal usando la base de datos GEO.

Resultados

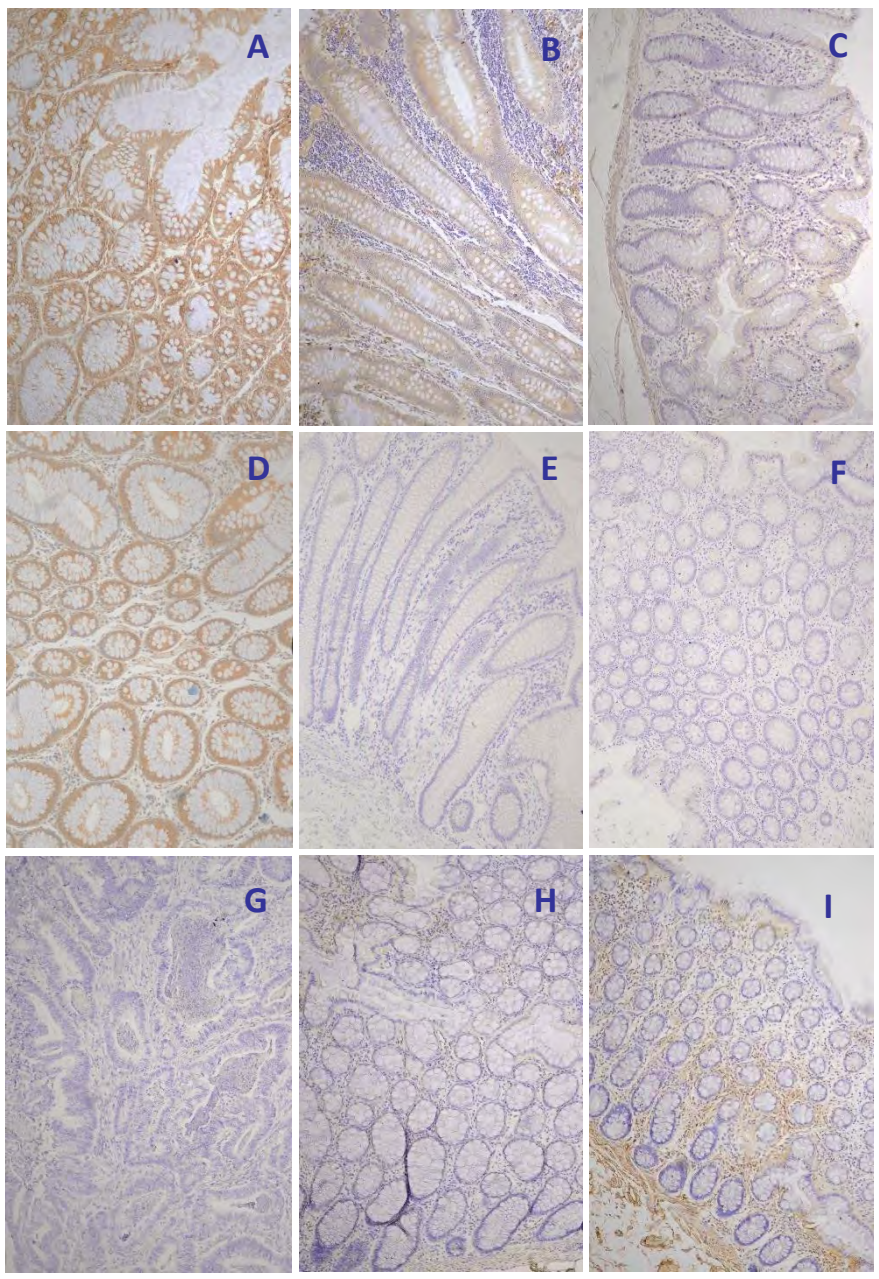

De las proteínas antioxidantes estudiadas, se observó que la intensidad de tinción de SOD2 era mínima en los colonocitos de tejido normal, aumentaba en el tejido inflamatorio peritumoral y era máxima en el tejido tumoral. La intensidad de SIRT3 también fue mayor en el tejido tumoral, mientras que la intensidad de UCP2 cambió en tejido inflamado y tumoral.

Los niveles de SIRT3 altos se asociaron a una peor supervivencia total de los pacientes, mientras que niveles de UCP2 altos se asociaron a un incremento en la supervivencia libre de enfermedad.

Figura 1. *Imágenes representativas de los resultados obtenidos por IHQ. A) SOD2 tejido tumoral; B) SOD2 tejido inflamado; C) SOD2 tejido sano. D) SIRT3 tejido tumoral; E) SIRT3 tejido inflamado; F) SIRT3 tejido sano. G) UCP2 tejido tumoral; H) UCP2 tejido inflamado; I) UCP2 tejido sano.*

Conclusión

SOD2 podría ser una proteína importante a la hora de evaluar la progresión del cáncer colorrectal y caracterizar la biología del tumor. Sin embargo, se hace necesario validar estos resultados en una cohorte mayor.

Agradecimientos

This work was supported by Projectes intramurals Synergia (SYN18/08); a grant from Programa postdoctoral Margalida Comas - Comunidad Autónoma de las Islas Baleares (PD/050/2020) and Miguel Servet Program (MS19/00201), Instituto de Salud Carlos III (ISCIII), Madrid.

Deciphering the potential of tumor-infiltrating circulant immune cells lipidomic characterization in CRC.

Karim Pérez-Romero[1], Albert Maimó-Barceló[1], Ramón M Rodríguez[1], Paloma de la Torre[3], Lucía Martín-Sáiz[2], José Andrés Fernández[2] Gwendolyn Barceló-Coblijn[1], Daniel H. Lopez[1]

1. Balearic Islands Health Research Institute (IdISBa), Spain; 2.Dep. of Physical Chemistry, University of the Basque Country (UPV/EHU), Leioa, Biscay, Spain; 3.Gastroenterology Unit, Hospital Universitari Son Espases, Palma, Balearic Islands, Spain

Introduction & Aims

Despite progress made in the colorectal cancer (CRC) field, the increase of the overall survival for patients in advanced stages remains still elusive. Therefore, besides improvements in the identification of emerging biomarkers for early detection, the development of new patient stratification tools and new immunotherapeutic treatments for the disease becomes essential. Remarkably, several studies have shown that the tumor microenvironment (TME) plays a crucial role in CRC progression. In this context, this study aimed to lay the groundwork for the characterization of the membrane lipid fingerprint of circulating immune cells of healthy donors and CRC patients, which eventually may infiltrate the tumor and play a pivotal role in tumor immunosurveillance.

Methods

The sample collection for this study was specifically approved by the Ethics Research Committee of the Balearic Islands (IB 3587/17 PI). Blood samples were obtained from 5 CRC patients and 5 control patients, enrolled at the Gastroenterology Services (IB 3350/16).

Peripheral blood immune cells were obtained after blood centrifugation. Subsequently, circulating $CD3^+/CD4^+$ (CD4+ Lymphocyte), $CD3^+/CD8^+$ ($CD8^+$ Lymphocyte), $CD3^-/CD56^+$ (NK Cell), $CD3^+/CD56^+$ (NKT Cell), $CD3^-/CD14^+$ (Monocyte), $CD66b^+$ (Neutrophil) and $CD3^-/CD19^+$ (B Cell) cells were isolated by Fluorescent Activated Cell Sorting (FACS).

Sorted immune cells (100.000 cells) were applied on poly L-lysine coated glass slides and analyzed by Matrix-Assisted Laser Desorption Ionization mass spectrometry (MALDI-MS).
In addition, a new methodology to detect tumor-infiltrating small populations of immune cells was developed (see Figure1).

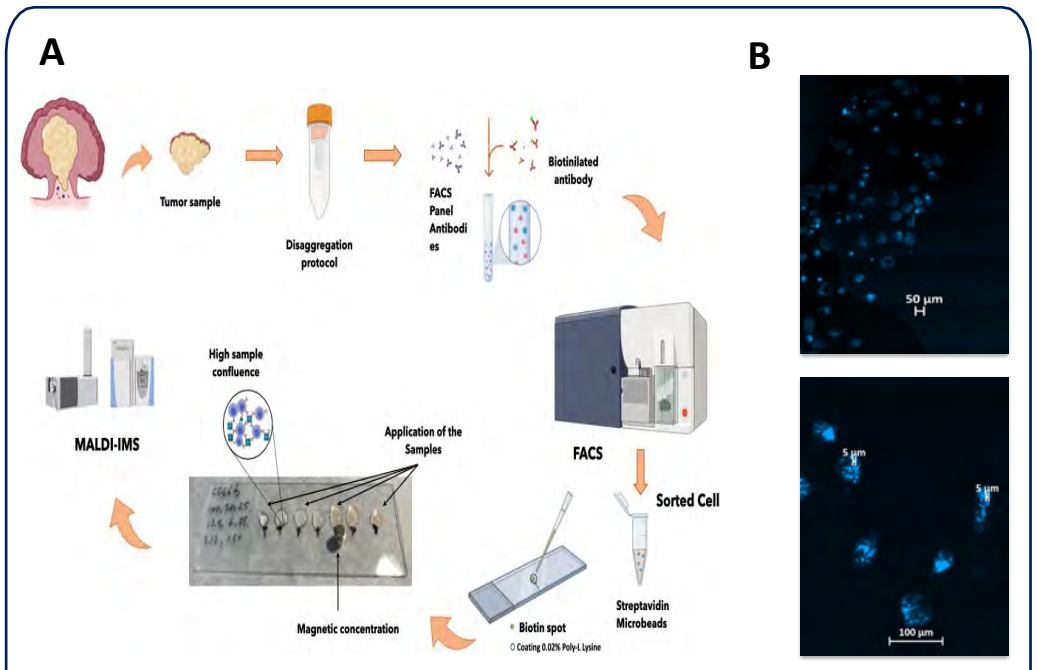

Figure 1. Sample preparation protocol for the detection of isolated cells using MALDI-IMS. A.Schematic representation of the methodology followed to achieve a high confluence of the sorted cells. B. Confocal microscopy images showing DAPI staining of $CD4^+$ immune cells obtained by FACS forming aggregates (100 um) using the developed protocol (Lipid analysis not performed).

Results

Using the methodology developed to apply the cells on the poly-L-lysine we were able to establish the lipidome using at least 1 to 2 orders of magnitude fewer cells than it is usually used. The analysis allowed the characterization of the main membrane lipid species within circulating monocytes, NK cells, B and T lymphocytes, neutrophils, and NKT cells. First, such analysis revealed a distinctive pattern of lipid species distribution for every cell type, confirming the specificity of the lipid fingerprint and the accuracy of the lipidome for our proposal to describe the immune compartment that shapes the TME.

Furthermore, the comparison between the healthy controls and CRC patients revealed a significant turnover of arachidonic acid-containing phosphatidylethanolamine (PE) and PE-plasmalogens, that may be associated with the clinical condition.

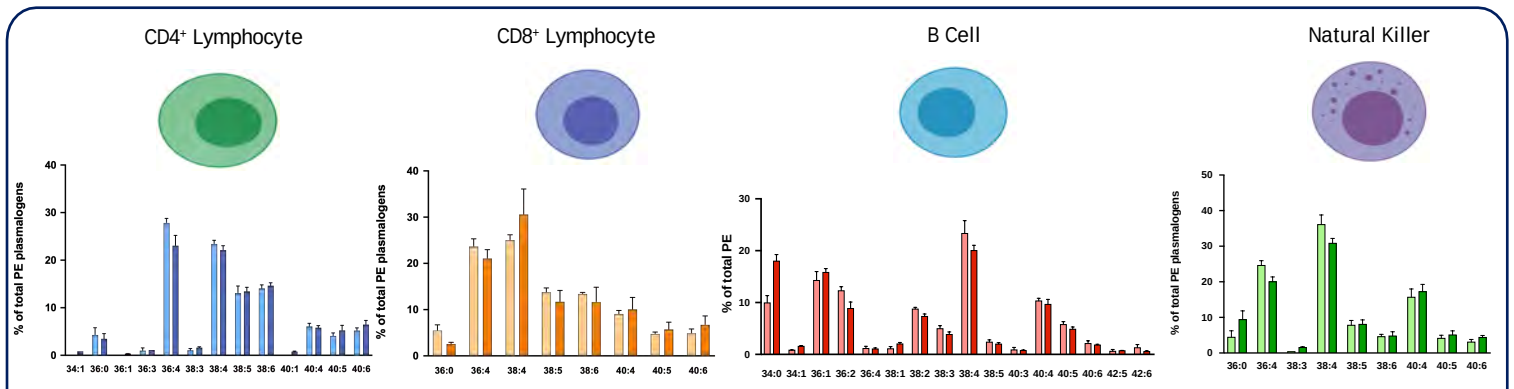

Figure 2. Membrane lipid composition of peripheral blood immune cells isolated from healthy donors and CRC patients. This data exhibit the significant changes detected in the lipid species composition within the PE and PE plasmalogens lipid classes under health conditions and in colorectal cancer disease. These changes are consistent with previous results published by our group, in wich a turnover of arachidonic acid-containing species has been documented in the lamina propria in the context of CRC[1,2]

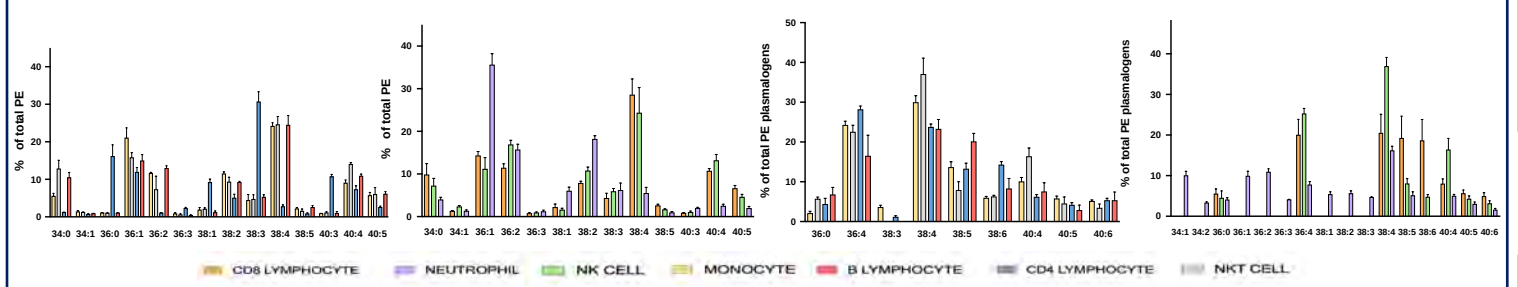

Figure 3. Membrane lipid composition in % of PE plasmalogens and PE for each of the isolated circulating-immune cell types. This representation illustrates the suitability of the lipid fingerprint for a thorough characterization of the TME, given that each immune cell type appears to present their intrinsic proportion of the main lipid species within these lipid classes.

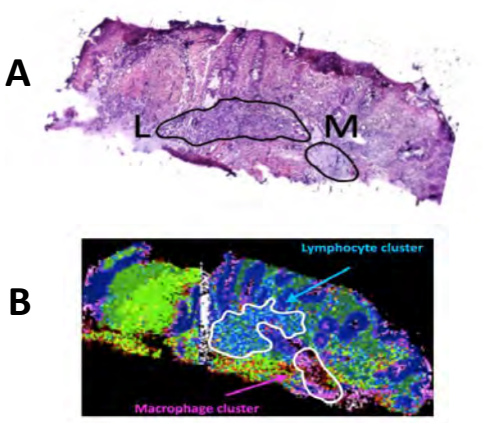

Figure 4. Histological sections of inflammed colon mucosa (ulcerative colitis patient). A. Hematoxilin and eosin stain betraying the presence of lymphocytic (L) and macrophage (M) infiltrates. B. MALDI-IMS analysis of the consecutive section revealed lipid clusters associated to each cell type, reinforcing the potential of the lipid fingerprint as a suitable tool to study the TME in colorectal cancer disease.

References

1. Bestard-Escalas, J., Garate, J., Maimó-Barceló, A., Fernández, R., Lopez, D. H., Lage, S., ... & Amengual, I. (2016). Lipid fingerprint image accurately conveys human colon cell pathophysiologic state: A solid candidate as biomarker. Biochimica et Biophysica Acta (BBA)-Molecular and Cell Biology of Lipids, 1861(12), 1942-1950.

2. Lopez, D. H., Bestard-Escalas, J., Garate, J., Maimó-Barceló, A., Fernández, R., Reigada, R., ... & Barceló-Coblijn, G. (2018). Tissue-selective alteration of ethanolamine plasmalogen metabolism in dedifferentiated colon mucosa. Biochimica et Biophysica Acta (BBA)-Molecular and Cell Biology of Lipids, 1863(8), 928-938.

Conclusions

- The setting up of this methodology has finally allowed the lipidomic characterization of sorted immune cells. Consequently, the increase in the sample size will have a direct impact on the robustness and the reliability of the results
- The molecular species relative abundance are intrinsic of each immune cell type, that is profoundly affected in patients with CRC. The methodology we have developed allows analyzing a smaller quantity of cells, providing the unique chance to analyze the lipidome of minor subsets of immune cells for the first time.
- The spatial resolution of MALDI-IMS allows the localization of lipid clusters that can be associated to specific cell types, opening chances for an unprecedent level of detail in a single histological section.

Acknowledgements

We are greatly thankful to the nurses and medical doctors of the Gastroenterology Unit of the Hospital Universitari de Son Espases (Palma, Spain).Funding: Institute of Health Carlos III (Miguel Servet Program, CP12/03338 & PI16/02200), Govern Balear (FPI/1787/2015), MINECO (RTC-2015-3693-1), Asociación Española Contra el Cáncer, Junta de Baleares(AECC 02/2017) co-funded by European Regional Development Fund.

Contact information: karim.perez@ssib.es
http://gwendybc22.wixsite.com/lipidshumanpathology

PAPEL DEL OXALIPLATINO SOBRE LA EXPRESIÓN DE LOS GENES MARCADORES DE CANCER STEM CELLS EN CÁNCER COLORECTAL

MARTINEZ-BERNABE, T[1]; MORLA-BARCELO, PM[1]; REYES, J[1,2]; OLIVER, J[1,3]; ROCA, P[1,3]; SASTRE-SERRA, J[1,3]; PONS, DG[1]

1 Grupo Multidisciplinar de Oncología Traslacional, Institut Universitari d'Investigació en Ciències de la Salut (IUNICS), Universitat de les Illes Balears (IdISBa), 07122 Palma, Spain. Instituto de Investigación Sanitaria Illes Balears, 07010, Palma, Spain.

2 Servicio Aparato Digestivo. Hospital Comarcal de Inca. Islas Baleares. Spain.

3 Ciber Fisiopatología Obesidad y Nutrición (CB06/03) Instituto Salud Carlos III, Madrid, Spain.

INTRODUCCIÓN

El Oxaliplatino (OXA) es uno de los fármacos quimioterapéuticos más utilizados para el tratamiento del cáncer colorrectal (CRC). De la misma manera que muchos agentes quimioterapéuticos, existe un porcentaje importante de recidivas después del tratamiento con OXA, el cual se ha asociado principalmente a la presencia de las Cancer Stem Cells (CSCs) en el tumor. Las CSCs, además de tener la capacidad de iniciar y mantener la progresión tumoral, presentan mecanismos metastásicos y de resistencias a los tratamientos convencionales con OXA.

MATERIALES Y MÉTODOS

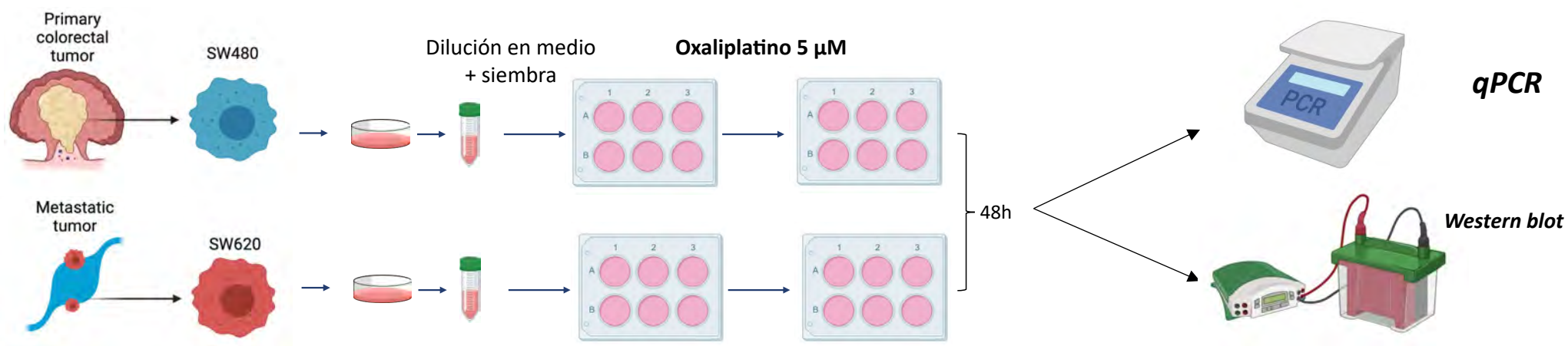

RESULTADOS

En ausencia de tratamiento, los genes marcadores de CSCs (SNAI2, ALDH, OCT4, ZEB1 y especialmente SOX2) se vieron sobreexpresados en la línea celular SW620 en comparación con la línea SW480. Los genes analizados aumentaron sus niveles de expresión con el tratamiento. Además, de la misma manera que en condiciones no tratadas, los niveles de expresión proteica de la Vimentina y la N-cadherina aumentaron en la línea SW620 en comparación a la línea celular SW480. El tratamiento también aumento los niveles de expresión proteica de la Vimentina en SW480 y de la N-cadherina en ambas líneas celulares.

***Tabla 1**. Efecto del tratamiento de Oxaliplatino sobre los niveles proteicos de Vimentina y N-cadherina después de 48h en SW480 y SW620. Se estudiaron las diferencias significativas después del análisis estadístico con ANOVA. L: Efecto línea celular; T: Efecto tratamiento; L*T: Efecto interactivo.*

	SW480		SW620		
Niveles de proteína (%)	***Control***	***Tratamiento***	***Control***	***Tratamiento***	***ANOVA***
N-cadherina	100 ± 27	181 ± 53	425 ± 115	1791 ± 525	L, T
Vimentina	100 ± 26	275 ± 73	6665 ± 602	5500 ± 590	L

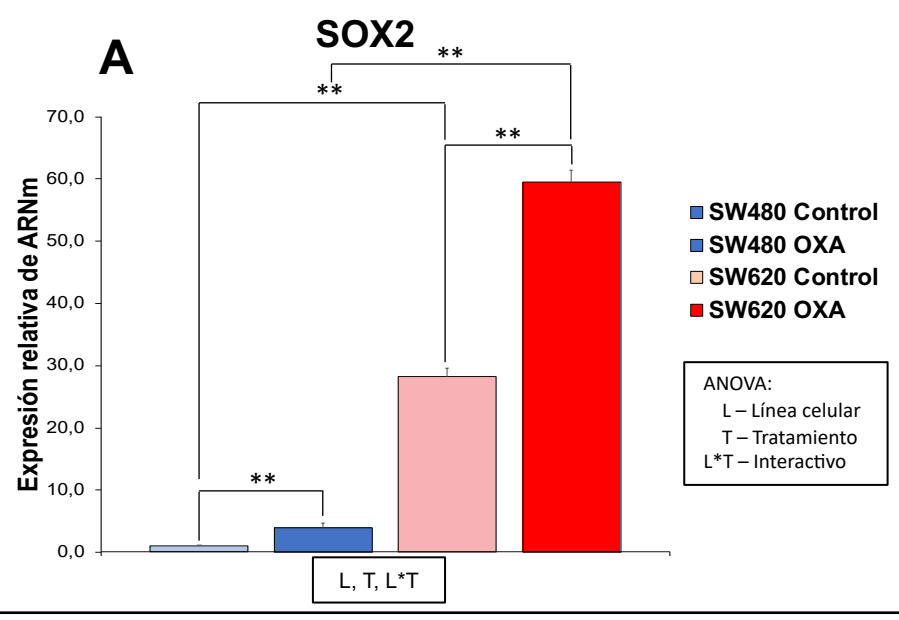

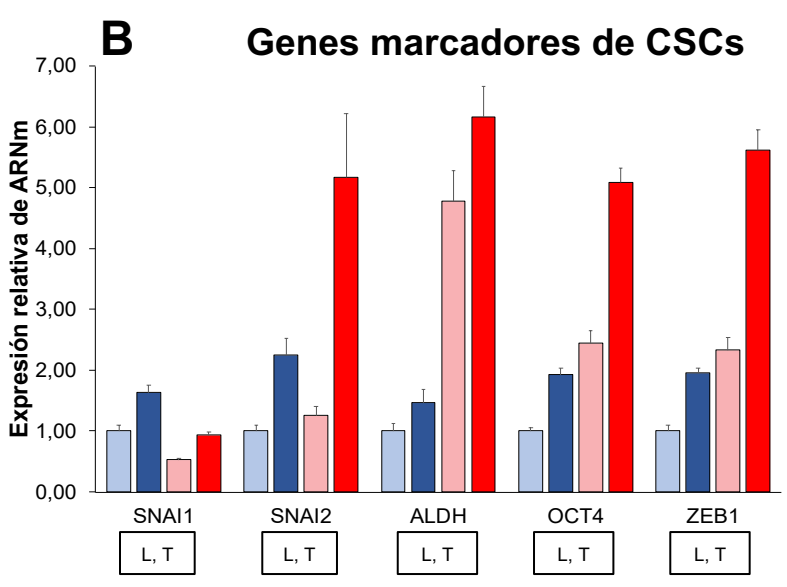

Figura 1. *(**A**) Expresión de SOX2 después de 48h del tratamiento con Oxaliplatino en SW480 y SW620. (**B**) Efecto del tratamiento con Oxaliplatino en la expresión de genes marcadores de CSCs (SNAI1, SNAI2, ALDH, OCT4 y ZEB1) después de 48h en SW480 y SW620. Se estudiaron las diferencias significativas después del análisis estadístico con ANOVA. L: Efecto línea celular; T: Efecto tratamiento; L*T: Efecto interactivo. Las diferencias significativas después del efecto interactivo fueron analizadas con t-student: ** p<0,01; * p<0,05.*

AGRADECIMIENTOS

Supported by Fundació Institut d'Investigació Sanitària Illes Balears (IdISBa)-Proyectos intramurales Programa "Primus" 2020 (PRI20/15). Ayuda Formación Personal Investigador FPI 2020 de la Consejería de Educación, Universidad e Investigación del Gobierno de las Illes Balears.

CONCLUSIÓN

Los resultados mostraron como las dos líneas celulares, bajo tratamiento con OXA, pueden iniciar una EMT aumentando la expresión de genes marcadores de CSCs y regulando los niveles de proteínas de EMT. En conclusión, este estudio destaca algunos genes marcadores EMT y CSC que podrían ser objetivos para comprender mejor las recidivas y resistencias al tratamiento con OXA en CRC.

Testing Wnt inhibitors in patient-derived primary cultures to combat soft tissue sarcomas

Marina Pérez-Capó[1,2], Elena Prados[3], Esther Martinez-Font[1,2], Rafael Ramos[3], Raúl Sánchez[2], Regina Alemany[1,4], Antònia Obrador-Hevia[1,5].

[1]Group of Advanced Therapies and Biomarkers in Clinical Oncology, Health Research Institute of the Balearic Islands (IdISBa), Palma de Mallorca, Spain; [2]Medical Oncology Department, Son Espases University Hospital, Palma de Mallorca, Spain; [3]Pathology Department, Son Espases University Hospital, Palma de Mallorca, Spain; [4]Group of Clinical and Translational Research, Department of Biology, University of the Balearic Islands, Palma de Mallorca, Spain; [5]Molecular Diagnosis Unit, Son Espases University Hospital, Palma de Mallorca, Spain.

Introduction

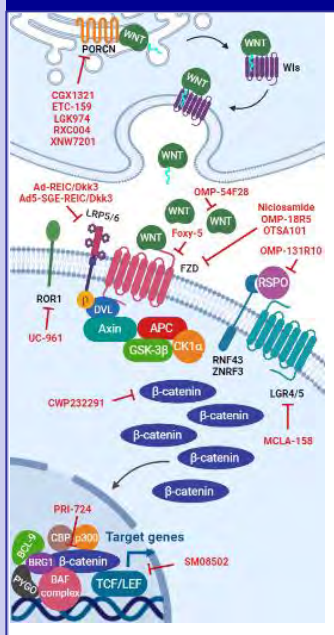

WNT signaling pathway and WNT inhibitors included in clinical trials.

Soft tissue sarcomas (STS) are a group of more than 50 histological subtypes of malignant mesenchymal tumours which represent less than 1% of all solid adult cancers. The poor prognosis of advanced STS makes the development of new therapeutic approaches a capital need. Our research group has a decade-long trajectory of translational studies in STS and has preliminary published data which point to a role of the Wnt signalling pathway as a therapeutic target that could complement current STS treatments.

The aims of this project were:

1) To generate a collection of STS patient-derived primary cultures for Wnt signalling pathway activation status characterization.

2) To test the antitumour efficacy of different Wnt inhibitors that are currently in clinical trials for other malignancies in order to combat STS.

Experimental design and methods

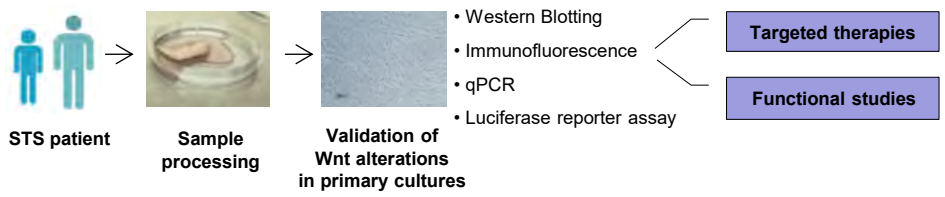

Figure 1. Project workflow.

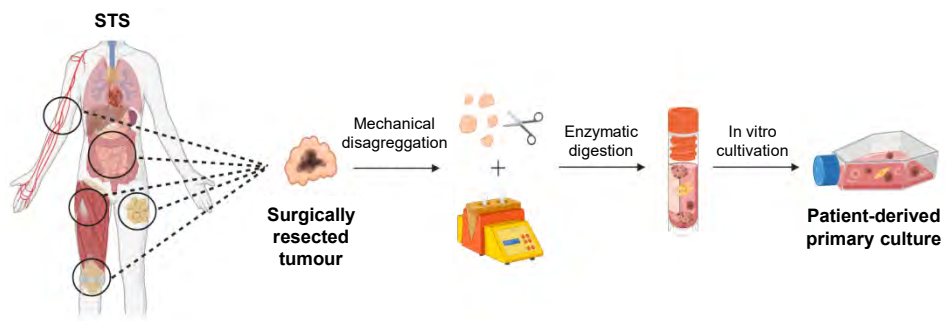

Figure 2. In vitro establishment of STS patient-derived primary cultures.

Results

1. Established collection of STS patient-derived primary cultures

A)

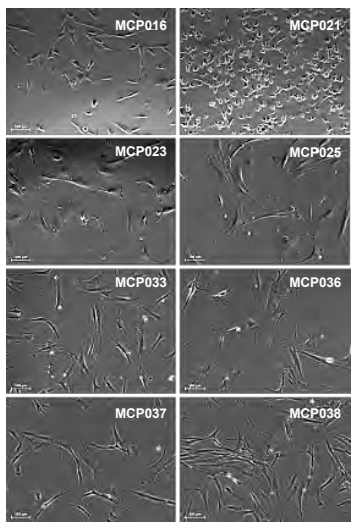

B)

Primary culture ID	STS subtype	Histological grade	Recurrence/ Metastasis
MCP016	Undifferentiated pleomorphic sarcoma	High	No
MCP021	Undifferentiated sarcoma	High	Metastasis
MCP023	Pleomorphic leiomyosarcoma	High	No
MCP025	Undifferentiated pleomorphic sarcoma	High	No
MCP033	Undifferentiated sarcoma fibrous histiocytoma-like	Intermediate	Recurrence
MCP036	Myofibroblastic sarcoma	Intermediate	No
MCP037	Synovial sarcoma	Intermediate-High	No
MCP038	Dermatofibrosarcoma protuberans	Intermediate	No

Figure 3. Morphological and histopathological characteristics of STS patient-derived primary cultures. A) Representative images of primary cell cultures at passage 10 taken with phase-contrast microscope Cell Observer (Carl Zeiss, Germany) with a 10X objective. **B)** Histopathological and clinical characteristics of the 8 tumours that we have managed to establish STS primary cultures for more than 10 passages. Histological subtypes and tumour grades were confirmed by an expert pathologist, Dr. Ramos.

2. Wnt signalling activation in STS primary cultures

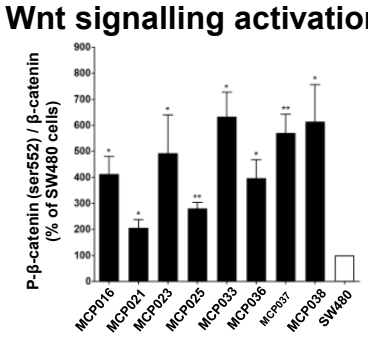

Figure 4. The active form of β-catenin is present in STS primary cells. Columns represent the ratio of P-β-catenin (Ser552) to β-catenin immunoreactivity. Each column is the mean ± SEM of 3 independent experiments normalized to SW480 cells (human colon cancer cell line). *P < 0.05, **P < 0.01.

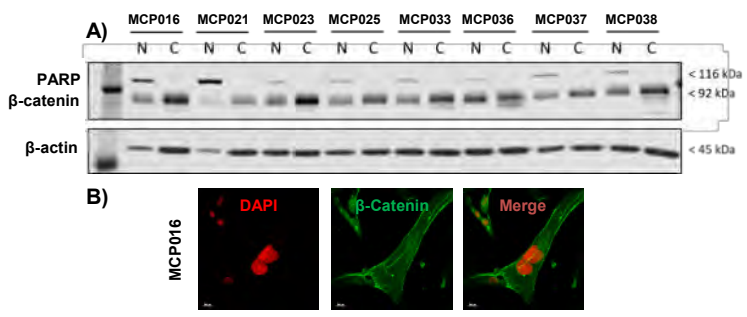

Figure 5. Nuclear β-catenin accumulation in STS primary cultures. A) Western blot of subcellular fractions. Antibodies used were β-catenin (Cell Signaling, #8480), PARP (#9542S) as nuclear marker and β-actin (#3700) as loading control. **B)** Cells were fixed in methanol:acetone (1:1) and stained with β-catenin (Cell Signaling, #8480). Alexa488 was used as secondary antibody and DAPI was added to visualize the nuclei.

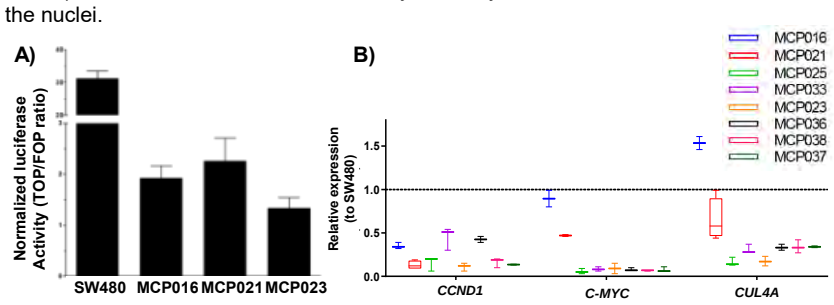

Figure 6. TCF/β-catenin-mediated transcriptional activation and expression of Wnt target genes in STS primary cells. A) Fold change of TCF/β-catenin-mediated transcription in primary cells respect to SW480 cells. TOPFLASH and FOPFLASH luciferase activities were measured after 24 hours of transfection and normalized to Renilla. Each column represents mean ± SEM of two experiments performed in triplicate. **B)** Expression levels of Wnt target genes assessed by qRT-PCR. Each value represents mean ± SEM of 3 experiments performed in duplicate relative to SW480.

3. Testing the antitumour efficacy of Wnt inhibitors on STS primary cultures

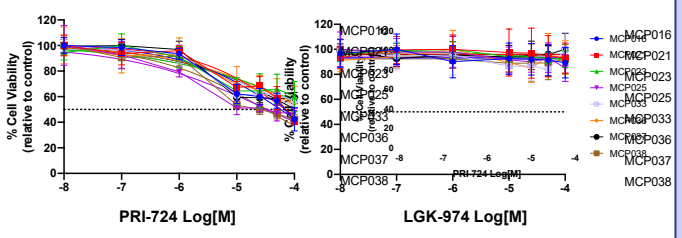

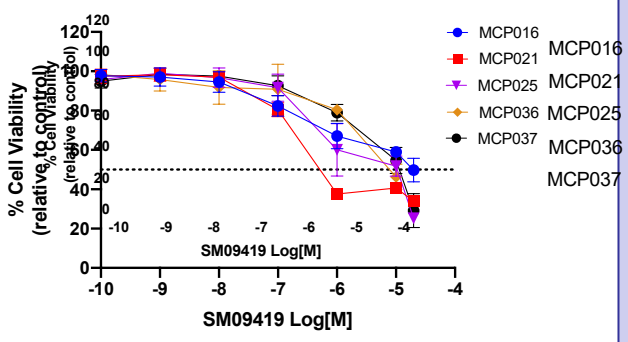

Primary culture	IC_{50} (uM) SM09419	PRI-724	LGK-974
MCP016	21.17	57.71	>100
MCP021	1.7	70.98	>100
MCP023	-	>100	>100
MCP025	4.99	33.97	>100
MCP033	-	>100	>100
MCP036	-	>100	>100
MCP037	8.96	>100	>100
MCP038	-	31.4	>100

Effect of Wnt inhibitors on STS primary cells viability. Cells were treated with PRI-724, LGK-974 or SM09419 (0.1-100 μM) and incubated for 48 hours. Cell viability was measured using the *CellTiter 96® AQueous One Solution Assay Kit*. Cell viability is represented as percentage relative to vehicle-treated cells and data is mean ± SEM of three independent determinations performed in triplicate. Table represents IC_{50} values of each drug calculated with Graphpad Prism 8.

Conclusions

1.Canonical Wnt signalling is highly activated in STS primary cultures.

2. SM09419 inhibits cell proliferation of STS primary cultures and is a promising therapeutic strategy for STS patients whose antitumoural effects has to be better characterized.

marina.perez@ssib.es

Fundación Mari Paz Jiménez Casado
G.E.I.S.
Illes Sostenibles
Institut d'Investigació Sanitària Illes Balears IdISBa
Son Espases hospital universitari

Exploring the transcriptomic regulation of MALDI-IMS membrane lipid distribution in human colonocyte differentiation and colon cancer

Albert Maimó-Barceló[1]; Joan Bestard-Escalas[1]; Karim Pérez-Romero[1]; Lucía Martín[4]; Jone Garate[4]; Daniel H. Lopez[1]; Marco Martinez[1,2]; Gonzalo P. Martín[1,3]; José M. Olea[1,3]; José A. Fernández[4]; Gwendolyn Barceló-Coblijn[1*]

[1]Health Research Institute of the Balearic Islands (IdISBa); [2]Pathological Anatomy Unit, Hospital Universitari Son Espases (HUSE) [3]Digestive and General Surgery Unit, HUSE, Palma, Spain; [4]Univeristy of the Basque Country, Leioa, Spain.

Background:

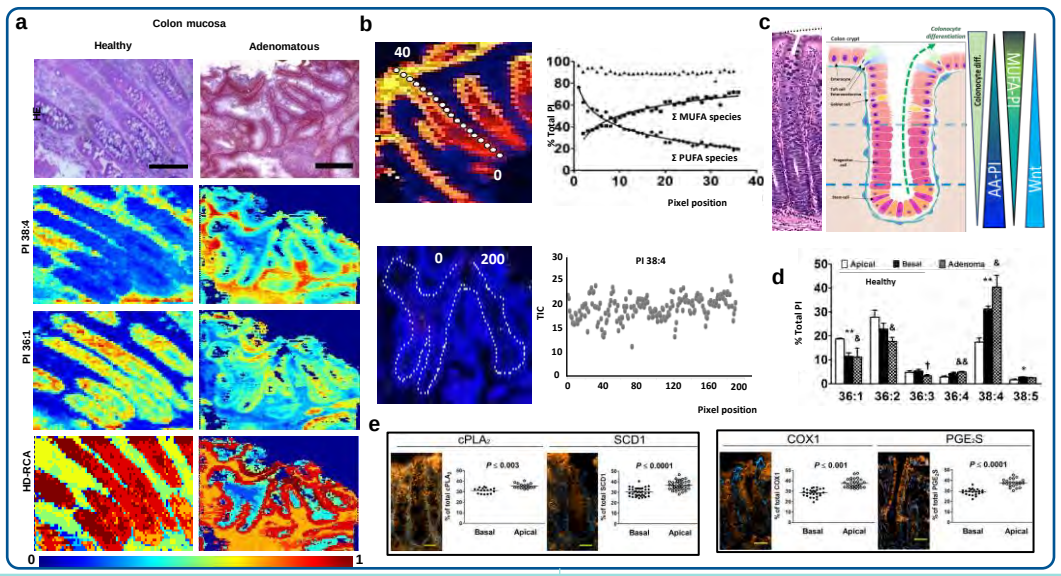

Figure 1. Colon crypt differentiation model: the AA- and MUFA-containing phospholipids and the colonocyte fate. (a) H&E stain of 10 µm colon histological section of healthy and tumor tissue, followed by the distribution of PI 38:4 & PI 36:1 molecular species, respectively, and Hierarchical Division-Rang Compete Clustering analysis (10 segments). **(b)** Pixel-by-pixel analysis of phospholipid composition in healthy and adenomatous mucosa: the PI shows a very specific regulation according to the process of cell differentiation. **(c)** Described Monounsaturated fatty acids (MUFA)-containing & Arachidonic acid (AA)-containing phospholipids gradient along colon crypts according to colonocyte differentiation state. **(d)** Clustering analysis enable to compares the statistical diff. between healthy epithelial regions and adenomatous epithelium, identifying an increase in AA-containing species in detriment of MUFA-containing species of PI. **(e)** Expression Key lipid enzymes in healthy crypt by IF. Scale bar = 50 µm.

Experimental design:

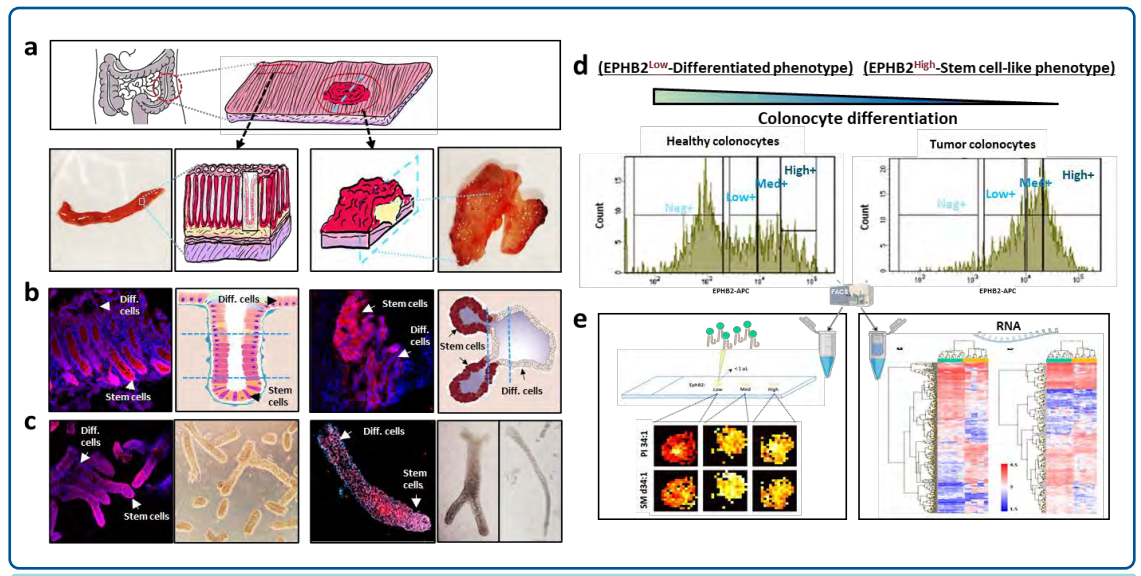

Figure 2. Isolating human colonocyte subpopulations. (a) Healthy and colon cancer adenocarcinoma patient derived crypts were isolated and disaggregated into single cells (n=5-8, T_{3-4}, N_{0-1}, M_0). **(b-c)** Immunofluorescence (IF) of EPHB2$^+$ (red) of histological sections (b) and isolated crypts (c) of human healthy and adenocarcinoma colon, DAPI (blue). The EPHB2$^+$ mark the stem cell-like phenotype. **(d)** The use of EPHB2 labeling, enabled the FACS according to the differentiation state of the cell (Neg-, Low-, Med-, High-EPHB2 subpopulations) (Merlos-Suarez *et al.* 2011). **(e)** Lipidomic and transcriptomic analysis of 15.000 colonocytes/EPHB2 subpopulation was performed for each pathological condition using MALDI-IMS (Neg ion mode, LTQ-Orbitrap XL, Thermo-Fisher Scientific) and gene expression microarray (Human Clariom S Pico, Thermo-Fisher scientific). IF images were acquired by confocal microscopy (LSM 710, Carl Zeiss).

Lipidomic results

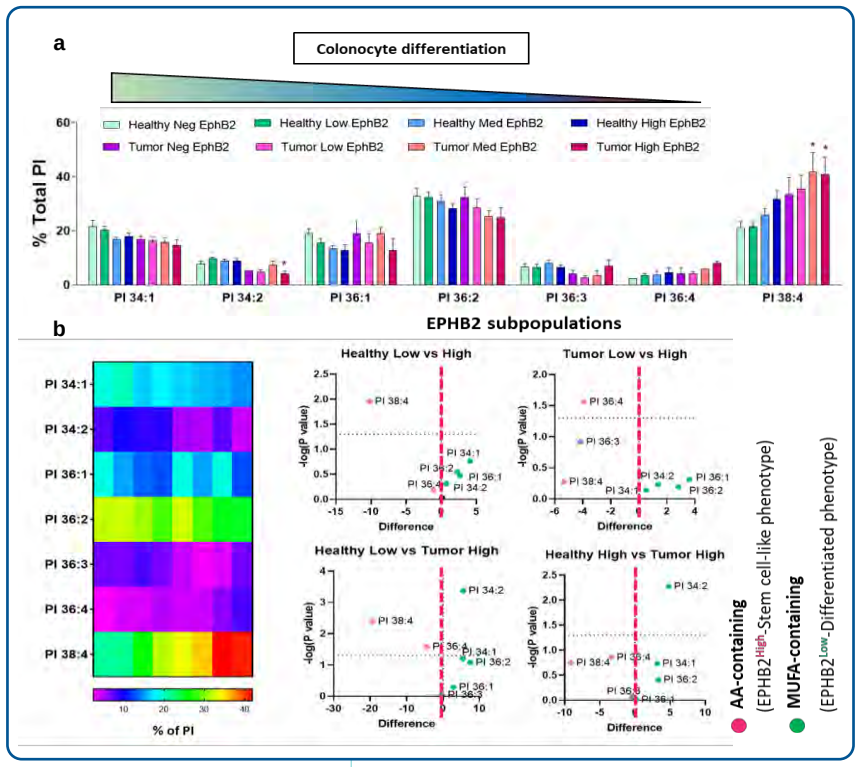

Figure 3. Lipidomic (n=6-8) results of healthy and tumor subpopulations. **(a)** % of molecular species distribution in PI recapitulates the distribution observed in tissue MALDI-IMS. **(b)** Multiple comparisons analysis of PI species confirms the association of AA-PI with the colon stem cells and the MUFA-PI with the differentiated colonocytes.

Transcriptomic results:

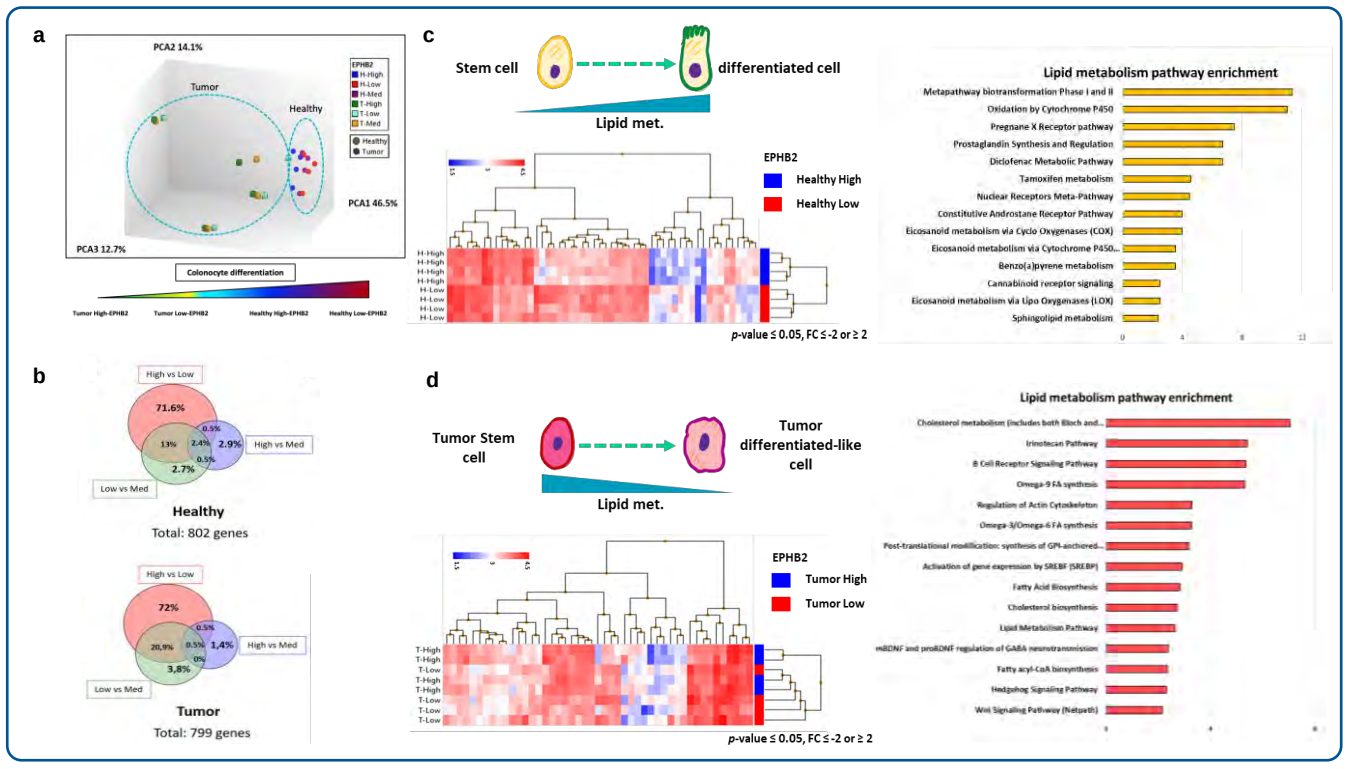

Figure 4 . Transcriptomic (n=4-5) results of healthy and tumor subpopulations.**(a)** PCA of gene expression array show pathological and differentiation state dependent sample distribution. **(b)** Differential expression analysis point to the High- vs. Low-EPHB2 as the best comparison to explain the process of cell differentiation. Pathway enrichment analysis of lipid metabolism for **(c)** healthy and **(d)** tumor colonocyte differentiation evidence and increased lipid metabolism in healthy diff. colonocytes, contrary to tumor colonocytes(Wikipathways) (p-value ≤ 0.05, FC ≤ -2 or ≥ 2).

Omics-data integration:

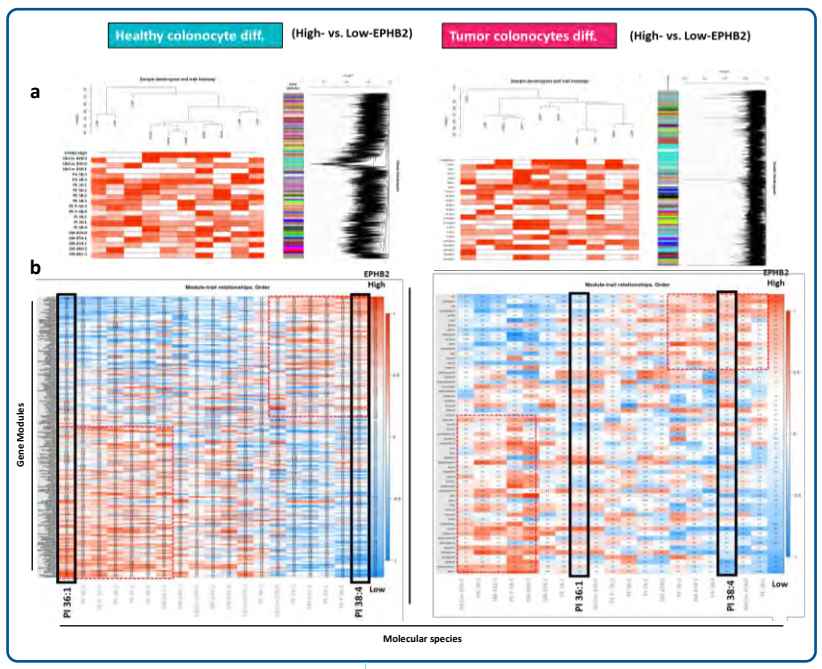

Figure 5 Lipidomic and transcriptomic data integration. (a) Transcriptomic data was analyzed using the R package for WGCNA (Langfelder P *et al.* 2008). Modules of genes were identified based on their expression patterns, identifying sets of genes with a high co-expression. **(b)** Molecular species with a significant differential expression were correlated with gene modules associated with High- or Low-EPHB2 phenotype, constructing a novel integrational matrix of lipid-RNA interaction. This multi-omic matrix enable the association of molecular species-specific phenotype in healthy or adenocarcinomatous differentiation with the better correlated transcriptomic regulation program.

Molecular species-specific gene network:

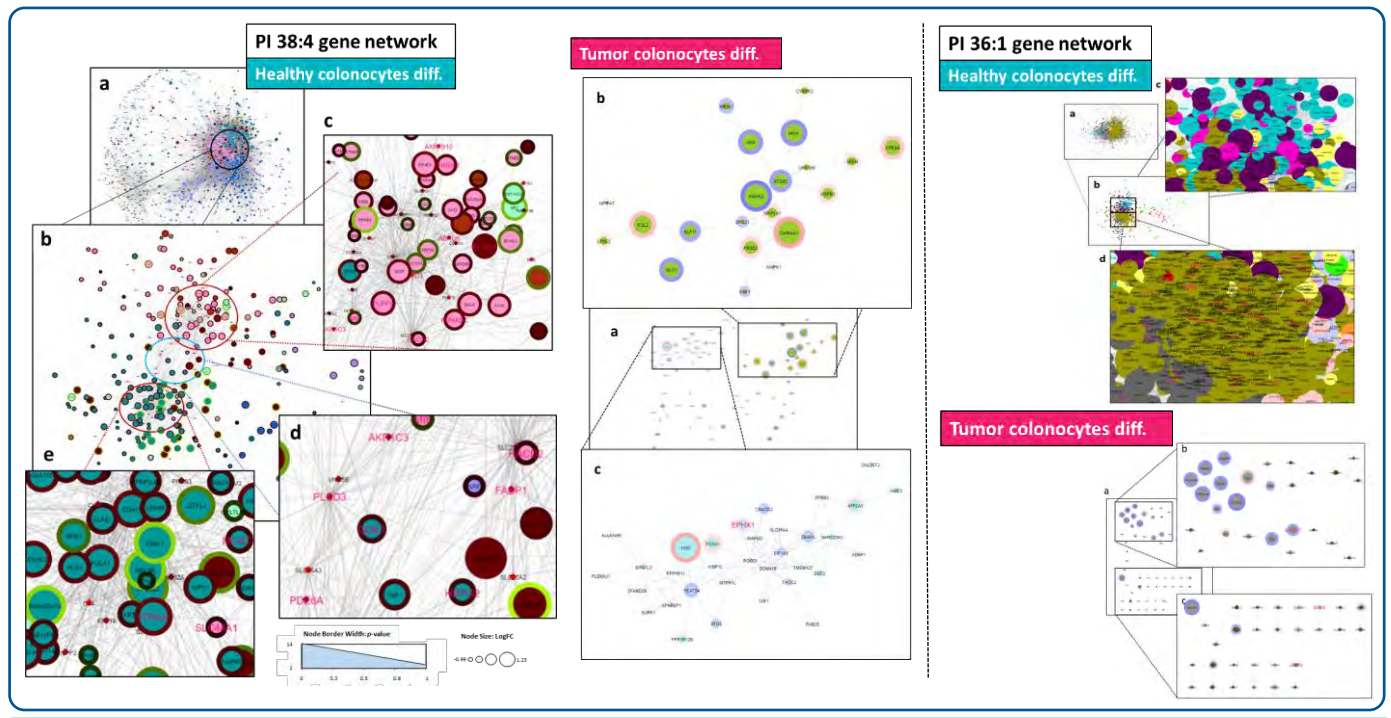

Figure 6. Transcriptomic network of PI 38:4 and PI 36:1 phenotype in healthy and tumor differentiation. Data for the two most significantly correlated molecular species in healthy crypt differentiation were extracted from the integration matrix for both pathological conditions. The gene modules that better explain the distribution of the **PI 38:4** and **36:1** were represented as a network. Further filtration by node weight-interaction enable the localization of potential gene regulators for each molecular specie, depending on the pathological condition (healthy networks, **a-d**; tumor networks, **a-c**). The lipidic genes coding for PLCD3, AKR1C3 and FABP1 were identified as interesting regulators of PI distribution in crypt homeostasis. Its expression is clearly down-regulated in tumor colonocytes. The complexity of PI 38:4 and 36:1 healthy networks is completely lost in tumor colonocytes. Node color = gene module; node size = fold change of High- vs. Low-EPHB2 subpopulations; Red genes = Lipid-related genes; node wight = p-value.

Summary:

1) The lipidomic results recapitulated the previously described MALDI-IMS gradients. Thus, AA-containing PI was more abundant in stem cells than in differentiated colonocytes, while MUFA-containing PI was oppositely distributed. Moreover, the PI 38:4 reinforced its increase in adenocarcinoma epithelium, specially in the stem cell subpopulation.

2) The lipid metabolism is differently regulated according to the pathological conditions: Prostaglandin metabolism as well as fatty acid biosynthesis is highly affected.

3) The transcriptomic network associated with regulation of PI 38:4 showed an elevated complexity in healthy crypts and identified several lipid genes (PLCD3, FABP1, and AKR1C3) highly implicated in the regulation of several gene modules. This complex regulation of PI 38:4 and PI 36:1 was lost in tumor colonocytes, which shows a reprograming of lipid metabolism according to its molecular signature.

4) Altogether these results, underscores the elevate versatility and reliability of the MALDI-IMS for the study of the lipid composition, and the detection of molecular alterations affecting specific cellular processes. Proving the sensitivity of the lipid fingerprint for different cellular proliferative states and pathological conditions. Also, evidence the need for a deeper understanding of lipid metabolism: even subtle phenotypic changes, may involve a large number of regulatory agents.

Acknowledgments:

Liquid biopsy in patients with peritoneal carcinomatosis of colorectal cancer

Evelin Horvath[1,2], Mónica Enver Sumaya[2], Juan José Segura Sampedro[3,4], Rafael Morales Soriano[3,4], María Nieves Esteve Perez[4,5], Aina Rosa Millán Pons[6], Pablo Luna Fra[1], Josefa Terrasa Pons[1,2], Antonia Obrador de Hevia[2,7], Mónica Guillot Morales[1,4]

[1]Medical Oncology Department, Son Espases University Hospital [2]Group of Advanced Therapies and Biomarkers in Clinical Oncology, Health Research Institute of the Balearic Islands (IdISBa) [3]Surgery Department, Son Espases University Hospital [4]Cirugia Oncológica Avanzada, m-health e Investigación Tecnológica Quirúrgica, Health Research Institute of the Balearic Islands (IdISBa) [5]Anesthesia and Resurrection Department, Son Espases University Hospital [6]Plataforma Suport Metodològic, Health Research Institute of the Balearic Islands (IdISBa) [7]Molecular Diagnosis Unit, Son Espases University Hospital, Palma, Spain

BACKGROUND/AIMS

Peritoneal carcinomatosis (PC) is diagnosed in 10-25% of metastatic colorectal cancer and has a very poor prognosis. Cytoreductive Surgery and Hyperthermic Chemotherapy (CRS-HIPEC) can be a curative treatment. There is an urgent clinical need for accurate tools to detect PC. The aim was to determinate the KRAS mutation by liquid biopsy, correlate the results with clinicopathological data of the patients in order to find a more sensitive biomarker of relapse for PC.

METHODS

Figure 1. Methological design

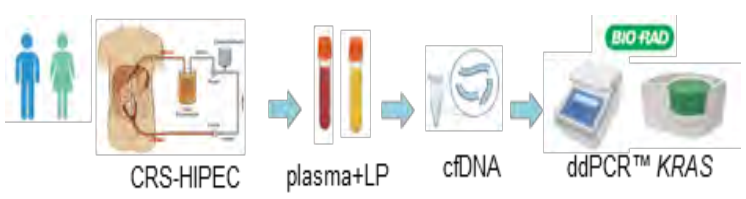

Plasma from ten healthy individuals was used as control.

Table 1. Patient characteristics

Factor		N:13
Gender	Male	5 (38%)
	Female	8 (62%)
Age (years)	66.1 (56-78)	
PCI	>10	6 (46%)
	<10	7 (54%)
Histology	Adenocarcinoma	10 (77%)
	Mucinous	3 (23%)
Sideness	Left	7 (54%)
	Right	6 (46%)
Liver metastasis	3 (23%)	
CEA (ng/ml)	>10	4 (31%)
	<10	8 (69%)
CA 19.9	>10	9 (69%)
	<10	4 (31%)

RESULTS

KRAS mutation was detected 100% of the peritoneal liquid (PL) (n=13) and 81% of plasma samples (n=11) **Fig.2.** Mutant allele fraction (MAF) medians were 0.284 (IQR 0.24 – 0.32) and 0.274 (IQR 0.11- 1.22) respectively, without significant correlation between both (R= -0.158; p=0.663) **Fig.3.** The cutoff value is 0.05 in case of plasma and 0.08 in case of peritoneal liquid. There was a moderate correlation (R=0.389; p=0.267) between MAF values of plasma and Peritoneal Cancer Index (PCI) **Fig.4**.

Figure 2. KRAS mutations detected (%) in plasma and peritoneal samples

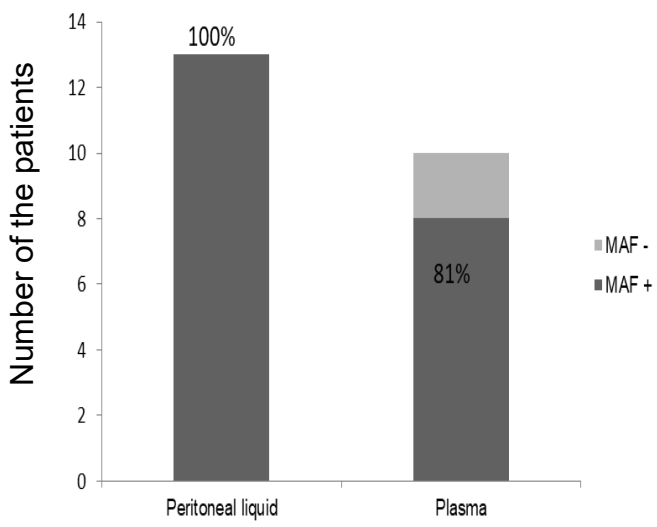

Figure 3. KRAS mutations values in plasma and peritoneal samples

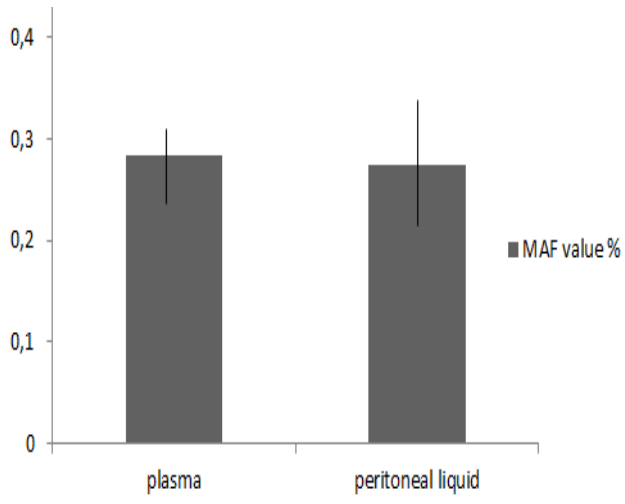

The overall survival (OS) of the patients was 36.95 months (IC 95% 15.22-58.67) and there was no significant correlation between MAF values and OS, neither the other clinicopathological parameters **Fig.5A**

Figure 4. Correlation between PCI and MAF in plasma samples

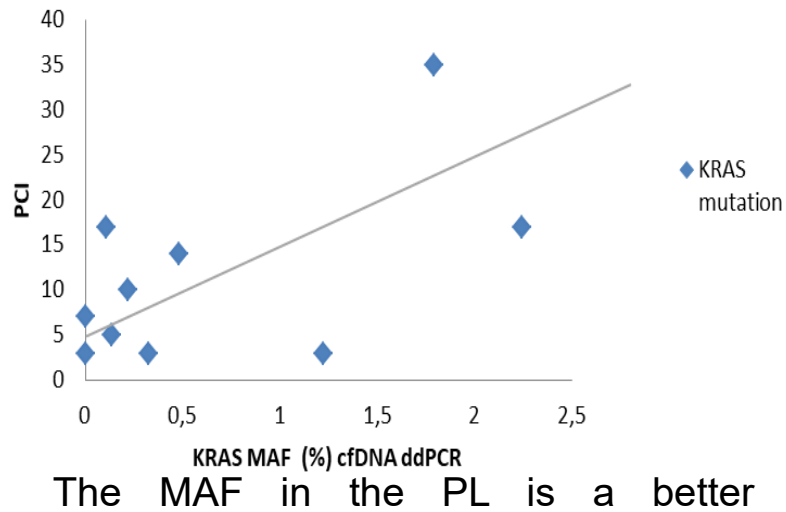

The MAF in the PL is a better biomarker for peritoneal carcinomatosis than plasma, with a positive predictive value of 83% and negative predictive value of 100% (cutoff 0,08) **Fig.5 B**

Figure 5.A Overall survival analysis B Curve ROC of MAF plasma/PL

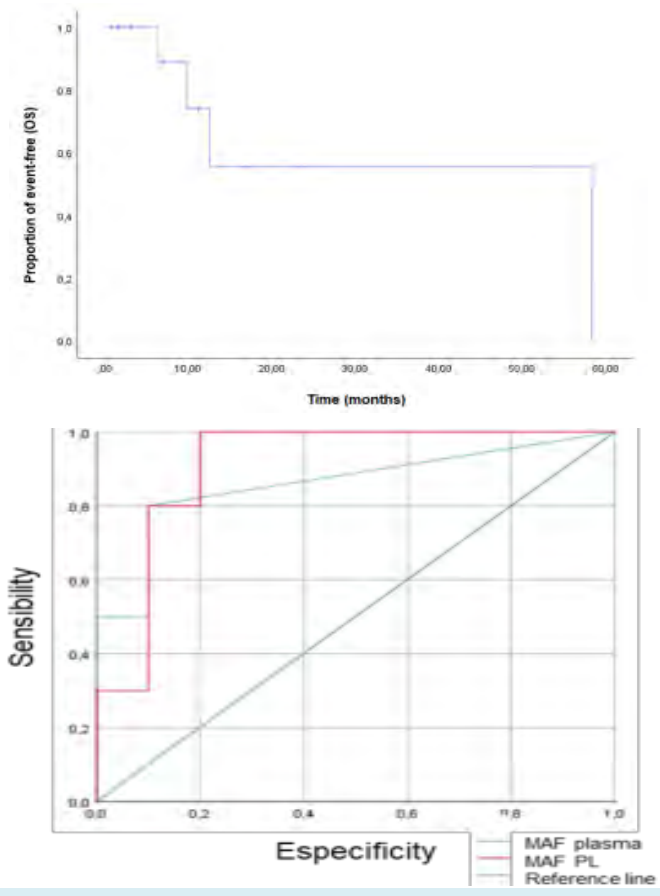

CONCLUSIONS

Our data on liquid biopsy in patients with CRC and PC suggest that it could be a sensitive method to detect mutations in both sample sources which could correlate with disease relapse and represent a novel prognosis biomarker. Further prospective studies are needed to confirm the clinical utility of liquid biopsy in these patients.

Characterization of mesenteric and peritumoral visceral adipose tissue of colon cancer patients: a multi-omic analysis of tumor the microenvironment

Maria Barceló-Nicolau[1], Alice Chaplin[1,2], Ramón M Rodríguez[1], Isabel Amengual[3], Álvaro García-Granero[4], Aina Ochogavia[4], Magdalena Coll[4], Andrea Craus[1,4], Sebastian Jeri[4], Gwendolyn Barceló-Coblijn[1]

[1]Health Research Institute of the Balearic Islands (IdISBa), Spain; [2]Consorcio CIBER, M.P. Fisiopatología de la Obesidad y Nutrición (CIBEROBN), Instituto de Salud Carlos III (ISCIII), Madrid, Spain; [3]Pathological Anatomy Dept., Hospital Universitari Son Espases (HUSE), Spain; [4]Digestive and General Surgery Dept., HUSE, Spain.

BACKGROUND

Colon cancer (CC) is the most frequently diagnosed malignant tumor in Spain and is among the most common malignant cancers worldwide. One of the main risk factors is obesity, whereby adipose tissue promotes the secretion of adipokines, cytokines and reactive species, which may lead to tumorigenesis. Visceral adipose tissue (VAT), which surrounds major organs, including the colon, has recently been associated to a range of diseases, including cancer (Fig. 1). Furthermore, evidence suggests that the tumor microenvironment may play a crucial part in carcinogenesis and proliferation. Our aim was to characterize the CC-associated adipose tissue at different tumoral stages using a multi-omic approach.

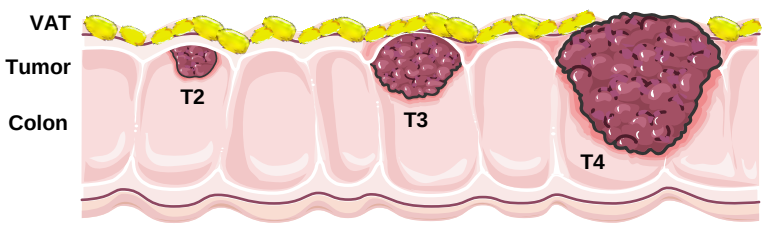

Figure 1. Representation of the localization of VAT in colon tissue with different tumoral stages.

METHODS

mVAT = mesenteric VAT
pVAT = peritumoral VAT

CC Patients

Tumor TNM stage
T2
T3
T4

SAMPLES	Anthropometric data	Blood	mVAT	pVAT
METHODS	• Age • Gender • Body mass index (BMI)	Adipokines/Cytokines (Luminex)	• Adipocytes → Lipidomics (UHPLC/MS) • Whole tissue → Transcriptomics	

RESULTS

Anthropometric data

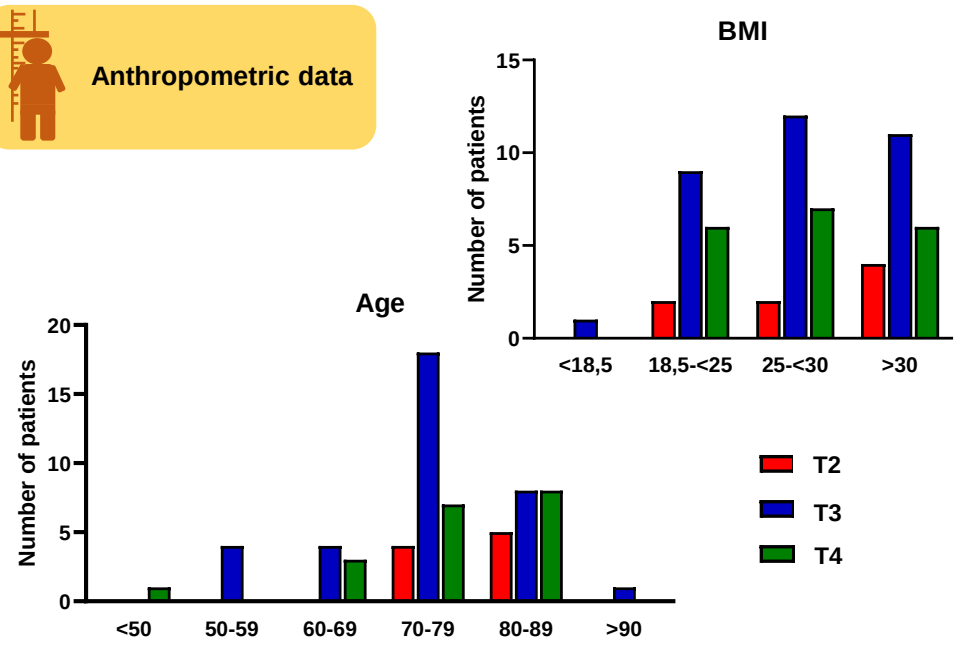

Figure 2. Representation of body mass index (BMI) and age of the patients included in the study. T2: n=9; T3: n=35; T4: n=19.

Blood samples

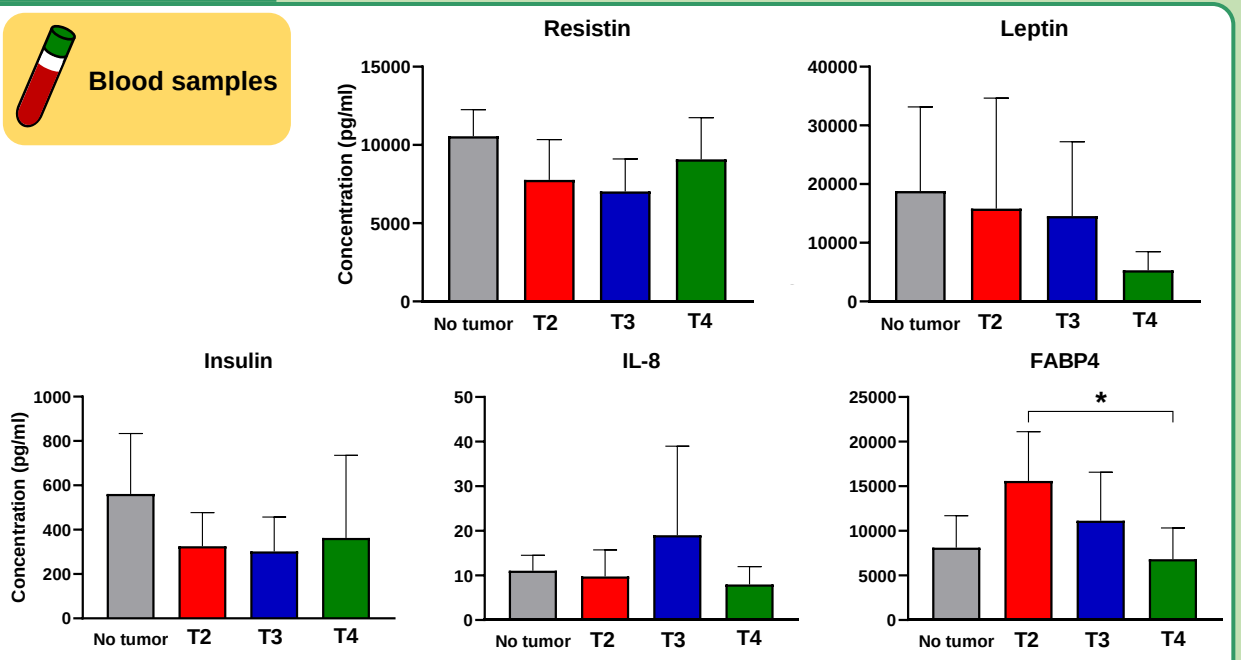

Figure 3. Plasma concentrations (pg/ml) of different cytokines and adipokines analyzed by Luminex. No tumor: n=3; T2: n=5; T3: n=8; T4: n=8.

mVAT adipocytes / pVAT adipocytes

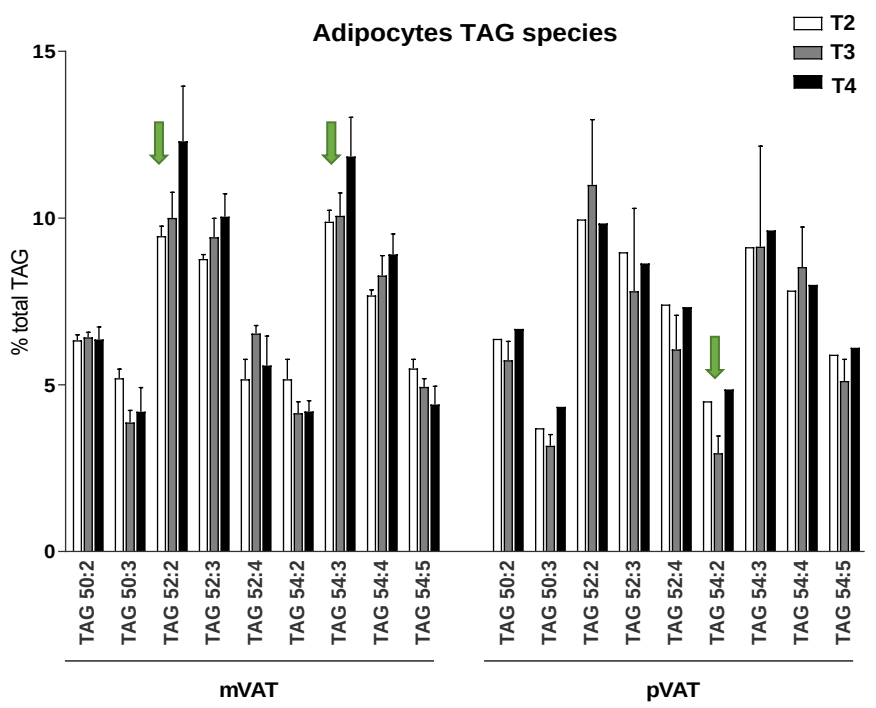

Figure 4. Lipidomic profile of most abundant molecular species of triacylglycerol (TAG) in mVAT and pVAT adipocytes from different tumoral stages. T2: n=3, T3: n=11, T4: n=4.

mVAT/pVAT whole tissue

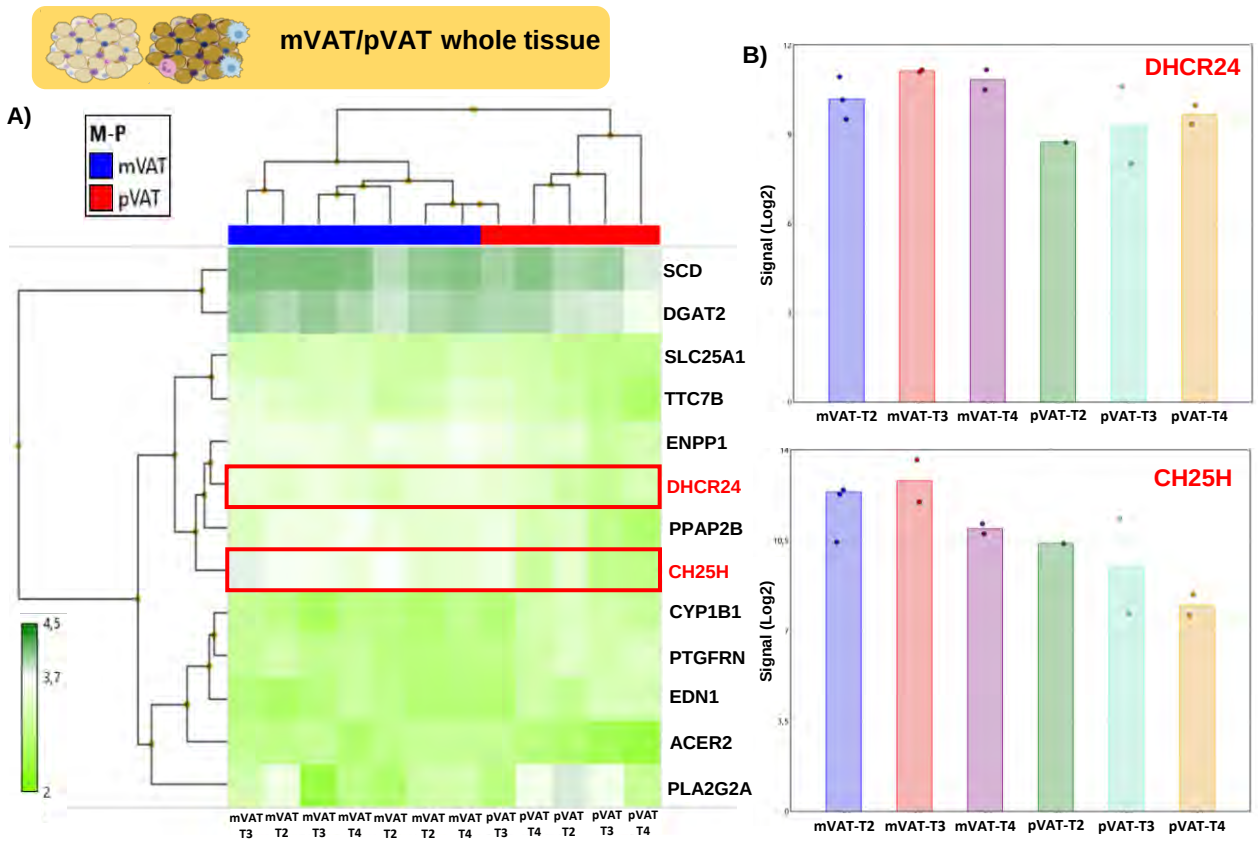

Figure 5. Transcriptomic analysis in whole adipose tissue. A) Non-supervised hierarchical clustering of lipid metabolism-related genes filtered by Fold Change >2 or <-2 and p-value<0,05. B) Differential expression of cholesterol 25-hydroxylase (CH25H) and 24-dehydrocholesterol reductase (DHCR24) gene in mVAT and pVAT. T2: n=4; T3: n=4; T4: n=4.

CONCLUSIONS

The different transcriptomic and lipidomic profile of VAT depending on its association to tumor (pVAT) or non-tumor (mVAT) cells reinforces the concept of a crosstalk between adipocytes and cancer cells, and thus highlights the importance of the study of the tumor microenvironment.

ACKNOWLEDGEMENTS

Finançat amb el fons de l'Impost del Turisme Sostenible del Govern de les Illes Balears

Contact information: maria.barcelonicolau@ssib.es

http://gwendybc22.wixsite.com/lipidshumanpathology

ZERO TOLERANCE TO SCIENTIFIC FRAUD
STOP IT. REPORT IT

Wnt/β-catenin and NF-κB pathways crosstalk in lung cancer.

Esther Martinez-Font[1,2]; Josep Muncunill Farreny[3]; Aarne Fleischer[3]; Mónica Enver-Sumaya[1,2]; Margalida Estava-Socias[4,5,6]; Cristina Gómez-Bellvert[1,7]; Ana Sofia de Freitas Matos Parreira[2]; Aitor Azkárate Martínez[1,2]; Jaume Sauleda Roig[5,8]; Antònia Obrador-Hevia[1,9].

[1]Group of Advanced Therapies and Biomarkers in Clinical Oncology, Fundació Institut d'Investigació Sanitària Illes Balears (IdISBa), Palma de Mallorca, Spain; [2]Department of Medical Oncology, Hospital Universitari Son Espases, Palma de Mallorca, Spain; [3]Genomic and Bioinformatics Unit, Fundació Institut d'Investigació Sanitària de les Illes Balears (IdISBa), Palma de Mallorca, Spain; [4]Centro de Investigación Biomédica en Red in Respiratory Diseases (CIBERES), Plataforma Biobanco Pulmonar CIBERES, Hospital Universitari Son Espases, Palma de Mallorca, Spain; [5]Group of Inflamation, repair and cancer in respiratory disease, Fundació Institut d'Investigació Sanitària Illes Balears (IdISBa), Palma de Mallorca, Spain; [6]Spanish Biobank Network, Instituto de Salud Carlos III, Madrid, Spain; [7]Department of Pathology, Hospital Universitari Son Espases, Palma de Mallorca, Spain; [8]Department of Pneumology, Hospital Universitari Son Espases, Palma de Mallorca, Spain; [9]Molecular Diagnosis Unit, Hospital Universitari Son Espases, Palma de Mallorca, Spain.

1. Background

Lung cancer is one of the leading causes of cancer death. Non-small cell lung cancer (NSCLC) represents 85% of all lung cancers and it is a lung cancer subtype with poor prognosis and low survival rates.

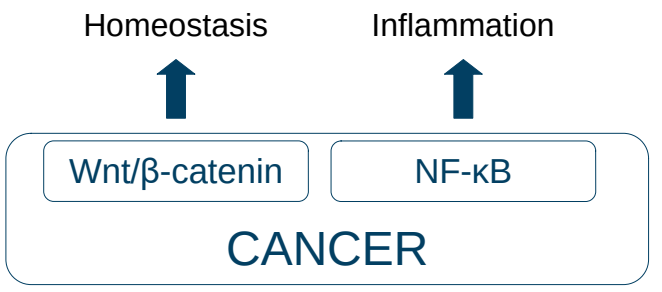

Wnt/β-catenin pathway is involved in several fundamental processes, whereas NF-κB is a major regulator of inflammation.

Aberrations within these two conserved pathways have been involved in several pathologies such as cancer.

2. Question

Which is the role of Wnt/β-catenin and NF-κB cross-regulation in NSCLC progression?

3. Methods

Clinical characteristics of NSCLC patients

	Adenocarcinoma	Squamous cell carcinoma	p.overall
	n = 23	n = 18	
Gender:			0,205
Male	18 (78,3%)	17 (94,4%)	
Female	5 (21,7%)	1 (5,6%)	
Age			0,276
years (Median, range)	67,0 [61,5 ; 69,8]	70,5 [63,2 ; 72,5]	
BMI			0,197
kg/m^2 (Median, range)	26,5 [24,2 ; 30,8]	24,0 [23,0 ; 28,5]	
Pack-years			0,439
(Median, range)	40,0 [24,0 ; 52,5]	50,0 [27,5 ; 60,0]	
Stage:			0,690
IA	4 (17,4%)	3 (16,7%)	
IIA	6 (26,1%)	4 (22,2%)	
IIIA	5 (21,7%)	7 (38,9%)	
IB	3 (13,0%)	0 (0,0%)	
IIB	4 (17,4%)	3 (16,7%)	
IIIB	1 (4,4%)	1 (5,6%)	

Selection of tumour tissue (n = 42)

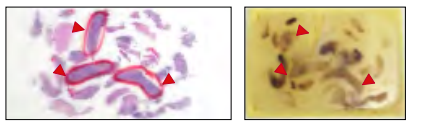

mRNA expression profile

GeneChip™ Clariom S

4. Results

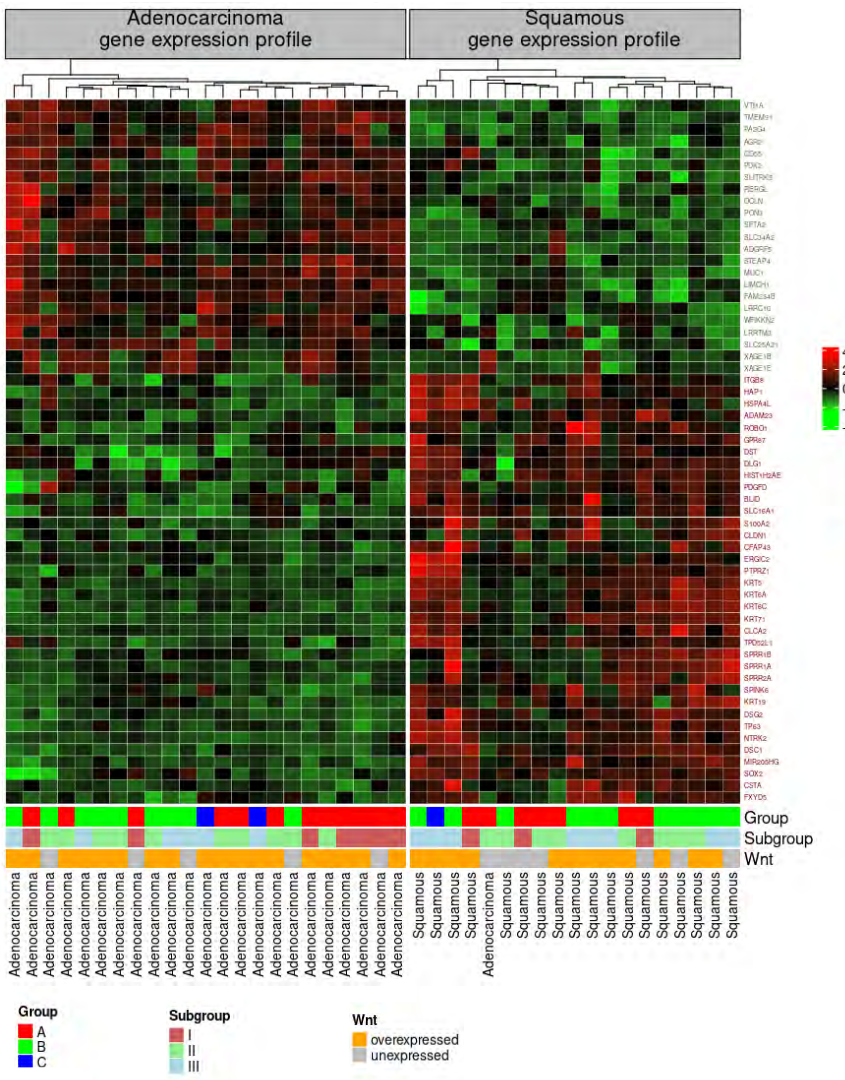

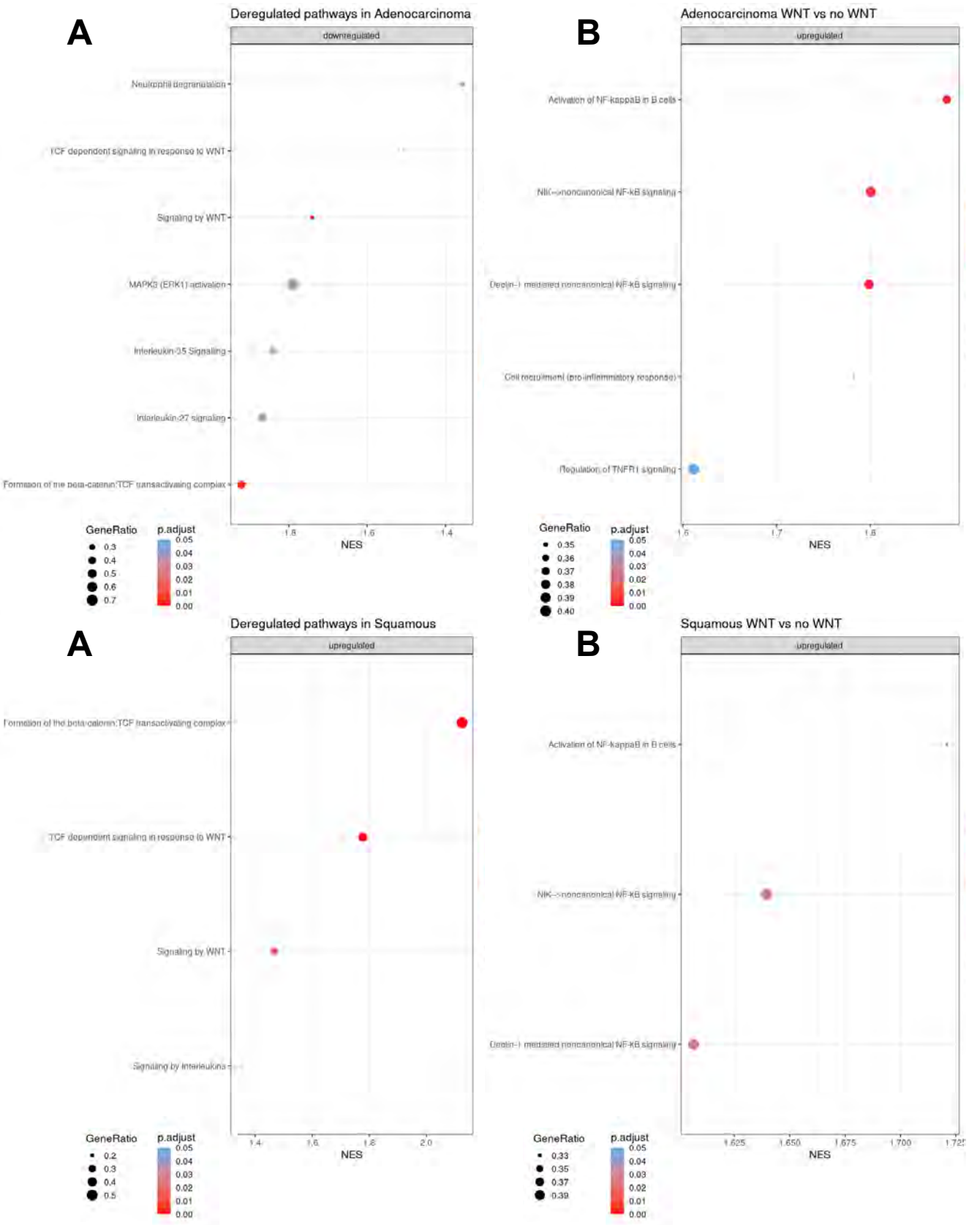

Figure 1 (Top Left). mRNA expression profile. Hierarchical clustering of differential gene expression significantly deregulated (|log$_2$FC| ≥ 0,6; adj.p-value ≤ 0,05) in adenocarcinoma vs squamous cell carcinoma. **(Right). Wnt/β-catenin and inflammatory processes implication in adenocarcinoma (Top right) and squamous cell carcinoma (Bottom right).** A) Enrichment analysis (GSEA) showing deregulated pathways related with Wnt/β-catenin and inflammatory processes in group B vs group A implemented by ReactomePA (Yu G, He Q (2016)). B) Enrichment analysis (GSEA) showing deregulated pathways related with inflammatoy processes in patients with Wnt/β-catenin overexpression vs patients with Wnt/β-catenin non-expression status implemeted by Reactome PA.

5. Conclusions

Better knowledge of mechanisms underlying Wnt/β-catenin and NF-κB pathways cross-regulation will provide potential prognostic biomarkers that enhance clinical management of NSCLC patients.

Institut d'Investigació Sanitària Illes Balears
IdISBa
Son Espases hospital universitari
esther.martinez@ssib.es